ZERO BRINE

D3.5: Report on the operation and optimization of the pilot system for the treatment of coal mine water

October 2020

Final

The ZERO BRINE project (www.zerobrine.eu) has received funding from the European Union's Horizon 2020 research and innovation programme under grant agreement No 730390.

Deliverable 3.5	Report on the operation and optimization of the pilot system for the treatment of coal mine water
Related Work Package	WP3 – Minimizing energy consumption and increase resource recovery yields through advanced treatment methods in the coal mine and textile industries
Deliverable lead	SUT
Author(s)	Krzysztof Mitko Marian Turek
Reviewer	Dimitris Xevgenos
Contact(s)	Krzysztof Mitko
Grant Agreement Number	730390
Funding body(ies)	European Union's Horizon 2020 Framework Program
Start date	1-June-2017
Project duration	48 months
Type of Delivery (R, DEM, DEC, Other)[1]	DEM = Demonstrator
Dissemination Level (PU, CO, CI)[2]	PU = Public
Date last update	6 October 2020
Approved by	Roelof Moll
Website	www.zerobrine.eu

Revision no	Date	Description	Author(s)
0.1	29/10/2018	First draft	Krzysztof Mitko (SUT)
0.2	06/05/2020	Version for the review	Krzysztof Mitko (SUT)
0.3	15/05/2020	Comments from reviewer	Dr. Dimitris Xevgenos (SEALEAU)
1.0	24/05/2020	Final version	Krzysztof Mitko (SUT)
1.1	06/10/2020	Revised upon comments external review	Krzysztof Mitko (SUT)

The ZERO BRINE project has received funding from the European Commission under the Horizon 2020 programme, Grant Agreement no. 730390.

[1] **R**=Document, report; **DEM**=Demonstrator, pilot, prototype; **DEC**=website, patent fillings, videos, etc.; **OTHER**=other

[2] **PU**=Public, **CO**=Confidential, only for members of the consortium (including the Commission Services), **CI**=Classified

Executive summary

One of the objectives of the ZERO BRINE project is to demonstrate the principles of circular economy in the coal mining industry. In order to do that, in the Subtask 3.1.4 of Work Package 3 (WP3), a pilot plant in the "Bolesław Śmiały" coal mine in Łaziska Górne, Poland, has been in operation from July 2019 to March 2020. The following report contains the results of the experiments performed during the pilot plant run. The tested system, as designed is WP3 Subtask 3.1.3 consisted of pretreatment, ultrafiltration, decarbonization, nanofiltration, reverse osmosis, and electrodialysis. Additionally, recovery of magnesium hydroxide was tested in both conventional precipitation with slaked dolime suspension and by crystallization with ion-exchange membrane (BCr-8 in the Polish BEC, and BCr-3 from the Italian BEC, respectively, developed in WP5, subtask 5.2.1). The recovery of sodium chloride using eutectic freeze crystallization has also been tested using BCr-1 crystallizer from Dutch BEC (WP5, subtask 5.2.1). The results were used to select the best variant of the proposed "ZERO BRINE" technology and compare it with the reference technology, used in "Dębieńsko" desalination plant in Czerwionka-Leszczyny, Poland. The calculated energy consumption and performance of the ZERO BRINE technology are to be used in WP7, subtask 7.1.4.

Contents

List of figures

List of tables

1. Introduction

a. Coal mine effluents & environmental problems

Coal mines comprise an important sector in the EU. Overall, coal is produced in 11 EU countries while it continues to make a major contribution to energy security in approximately half of the member countries. Further, coking coal has been identified as one of the 27 critical raw materials by the European Commission (EC), since the supply risk is high, linked to high concentration of supply in China and Australia and because its economic importance is calculated as high due to use in the metallurgy sector. As such, coal production will remain a very important sector in the future.

The coal mining industry is deeply affected by the environmental and economic problems with saline waste water disposal. The amount of salt discharged annually to the rivers in Poland by the mining sector is ca. 4 mln tonnes. Poland's two longest rivers (Vistula and Odra) are under significant pressures from mining activities. For many years excessive salt concentration has been found in the Vistula River, with 94% of the chlorides originating from hard coal mining activity. The Vistula River contains about 55 % of the total fresh water resources in Poland and covers about 60% of the water needs in the country (including the river basin). The salination of Vistula River is the cause of losses in industry, agriculture and water transport which are estimated to be $100-250 million per year.

b. ZERO BRINE project: WP3

The Work Package 3 of the ZERO BRINE project aims at demonstrating circular economy solutions in two process industry sectors: coal mining and textile industries. This includes two pilot plants, one in Poland (Task 3.1) and one in Turkey (Task 3.2), showing innovative brine treatment at pilot scale. The pilot plant in Poland is an integrated membrane system, using waste (coal mine) water to produce raw materials, including sodium chloride, magnesium hydroxide, calcium chloride, clean water and gypsum – see Figure 1. The pilot was based on the analyses of water chemistry of the coal mine water samples collected at the site (Subtask 3.1.1, see Deliverable 3.1), preliminary bench-scale experiments on nanofiltration, reverse osmosis, and electrodialysis (Subtask 3.1.2, see Deliverables 3.2 and 3.3), which allowed final design to be completed and the pilot equipment to be constructed (Subtask 3.1.3, see Deliverables 3.3 and 3.4). The preliminary work was done at 23.06.2019 (month M25 of the ZERO BRINE project).

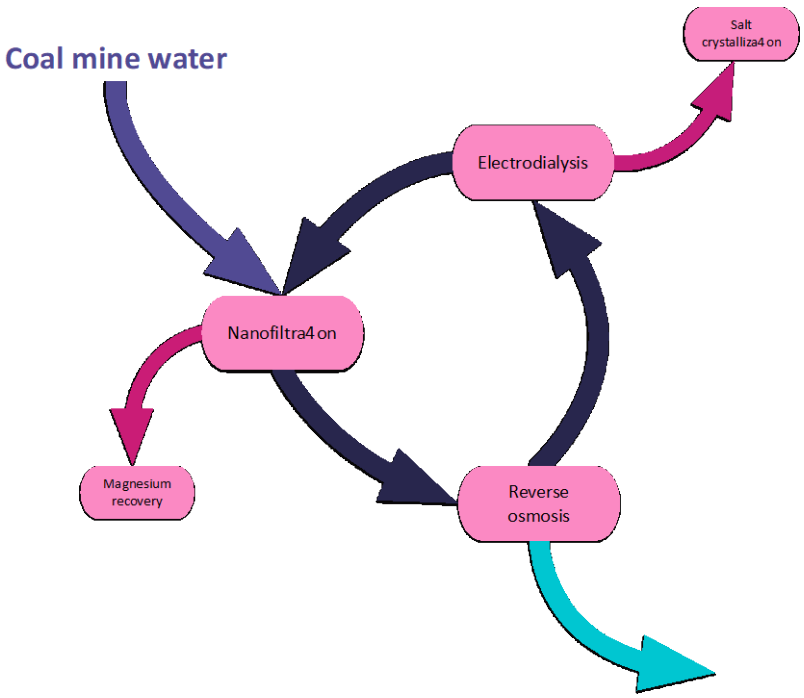

Figure 1 General scheme of the proposed approach to coal mine water treatment

The feed – coal mine water – after being pre-treated with ultrafiltration and decarbonization, is subjected to a two-pass nanofiltration treatment. Nanofiltration is a membrane method, which allows separation of univalent ions – such as sodium and chlorides – from bivalent ions – calcium, magnesium, sulphates. The nanofiltration unit thus splits the coal mine water into two streams: salt-rich permeate and calcium and magnesium-rich retentate. The retentate can be used for recovery of magnesium hydroxide, a valuable commodity in the refractory materials industry. The remaining calcium-rich solution could be used as a de-icing liquid. The nanofiltration permeate is concentrated in a hybrid reverse osmosis-electrodialysis system, which produces demineralized water of quality close to distilled water, highly saline concentrate, and the diluate, which can be recycled either before the reverse osmosis or before the nanofiltration. The highly saline concentrate could then be sold directly or used as a source for salt crystallization.

c. Scope of the deliverable

This deliverable presents the results from the operation and optimization of the pilot system developed by SUT. The system was installed on 23/06/2019 and has been operated during the period of 24/06/2019 to 16/03/2020.

The plant is located in ZG “Bolesław Śmiały” in Poland – a coal mine owned by PGG (Polska Grupa Górnicza S.A.), the EU largest black coal mining company, producing annually approx. 30 million tons of black coal (total EU production: ~100 million tons). The “Bolesław Śmiały” coal mine currently discharges over 730 000 m^3 of saline coal mine water annually – see Table 1. Since the salinity of coal mine water surpasses the legal limits, they mix the waters with industrial waste water from the energy plant sharing the same site. There currently is no further treatment of discharge, but because of the tightening environmental regulations, the company is seeking new methods for decreasing the salt load in their waste waters. The technology proposed in the ZERO BRINE project has the surplus value of extracting valuable products from the discharge: reverse osmosis permeate of high purity, which can be utilized in a nearby power plant, and inorganic compounds such as magnesium hydroxide and salt, which have commercial value.

Table 1 The amount of waste water and salt load discharged by "Bolesław Śmiały" (data from 2017)

Volume of coal mine water [m^3]	Average concentration of chloride + sulphates in coal mine water [mg/dm^3]	Average concentration of chloride + sulphates in discharge after mixing with industrial waste water [mg/dm^3]	Environmental fees, assuming 1€ = 4.5 PLN [€]
730 897.0	12 999.5	2 114.0	77 828.20

To assess the plant performance, the results obtained in the ZERO BRINE project were compared with the reference technology (see Figure 2 – data taken from Turek et al., Desalin. Water Treat. 64 (2017) 244-250): the desalination plant in Czerwionka-Leszczyny, Poland, formerly known as "Dębieńsko". The reference plant mixes saline mine water and reverse osmosis retentate from brackish water desalination. The brines are then concentrated using vapor compression method, and next the evaporated salt and gypsum are crystallized. Evaporators are powered with electrical energy, what makes their exploitation expensive; the energy consumption of brine concentrator (VC) is 44 kWh/m^3 of distillate, while the energy consumption of brine crystallizer is 66 kWh/m^3 of distillate. One of the goals of ZERO BRINE project is to show that applying the circular economy principles can decrease the energy consumption by 50% compared to the reference plant.

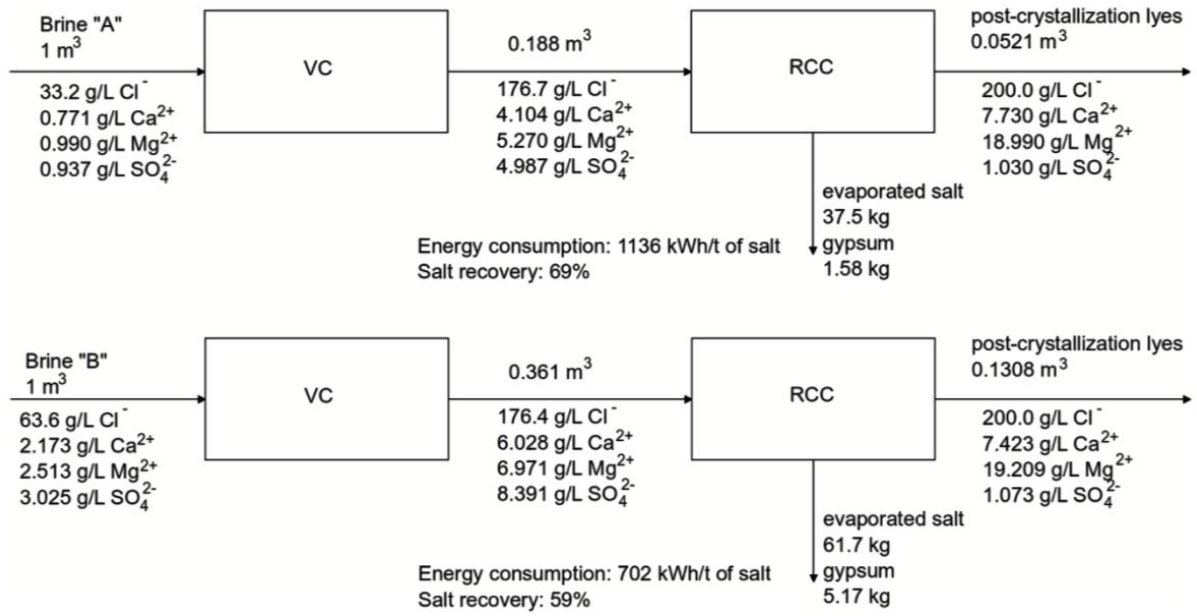

Figure 2 The process stream compositions and performance indicators for "Dębieńsko" plant working on two different brines (VC – vapor compression, RCC – crystallizer)

2. Technical design of the plant

Figures 3-10 present the final design implemented in the pilot plant, before further modifications took place. Instead of directly injecting hydrochloric acid into the feed stream, a weak ion-exchanger has been used for acidification. The unit operations tested in the plants were located inside two containers (see Figures 9 and 10) and connected as presented in Figure 11.

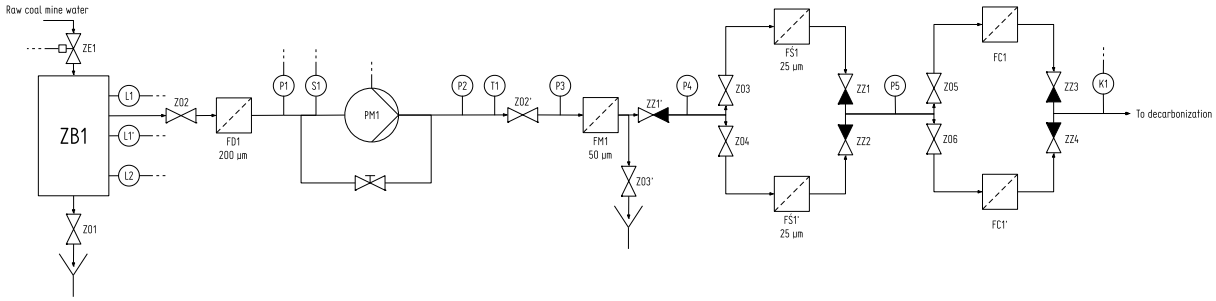

Figure 3 The plant pre-treatment unit (ZE – electro-valve, ZB – tank, ZO – drain valve, L – liquid level sensor, FD – slot filter, FM – bag filter, FŚ – candle filter, FC – carbon filter, ZZ – check valve, K – conductivity meter, P – manometer, S – dry run sensor, PM – pump, T – thermometer)

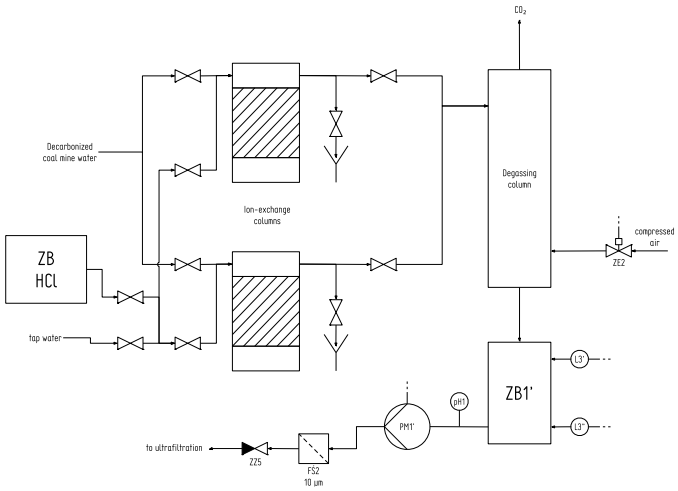

Figure 4 The plant decarbonization unit (ZB – tank, ZZ – check valve, FŚ – candle filter, ZE – electro-valve, pH – pH meter, L3 – liquid level sensor)

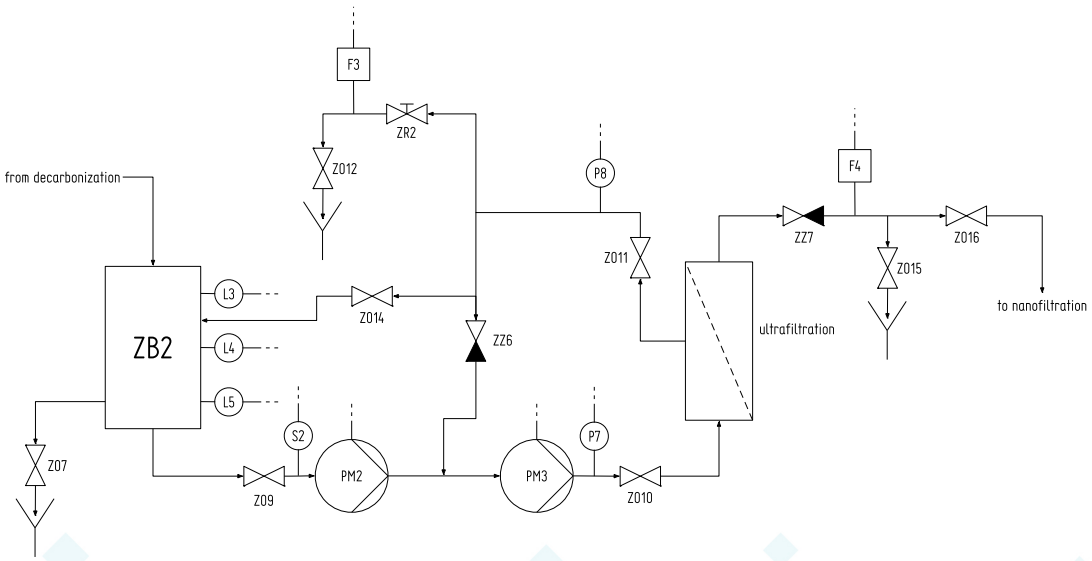

Figure 5 The plant ultrafiltration unit (ZB – tank, L – liquid level sensor, ZO – drain valve, F – flow meter, P – manometer, ZZ – check valve, PM – pump, S – dry run sensor, ZR – regulation valve)

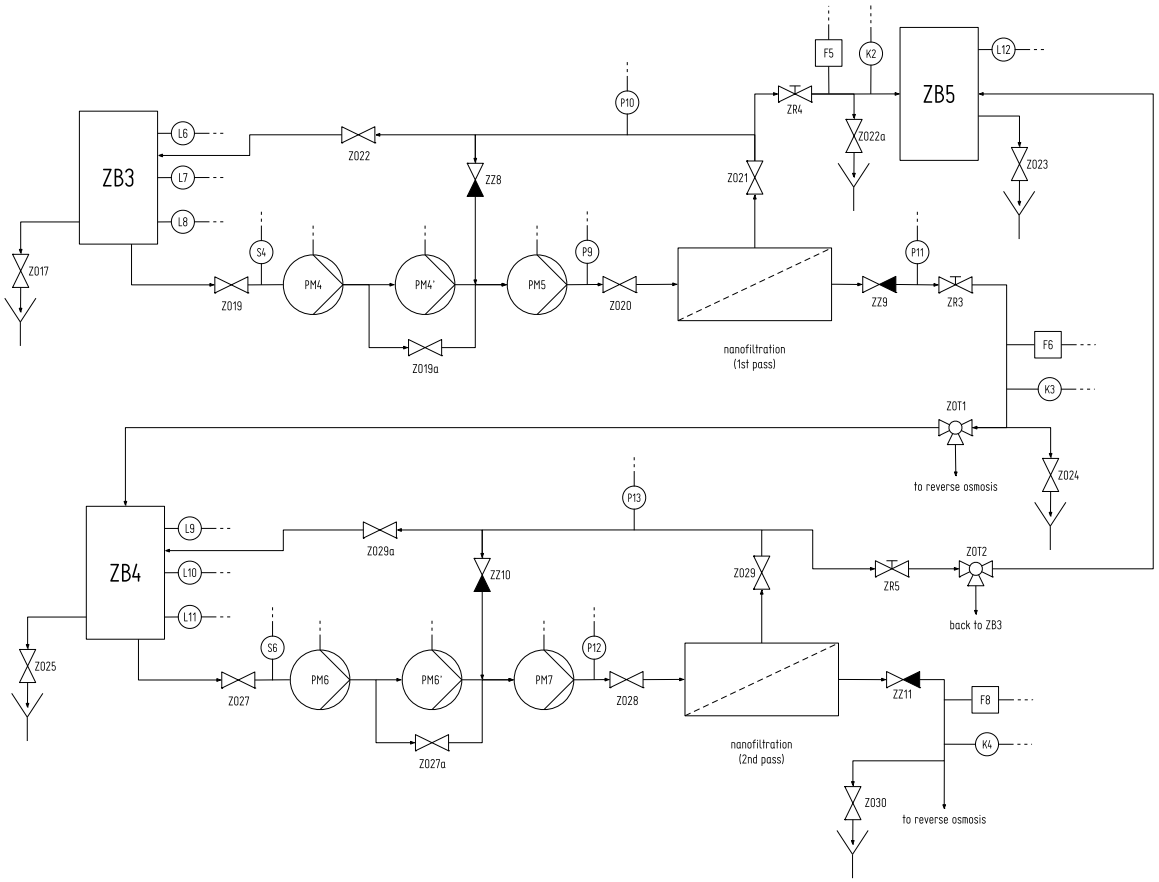

Figure 6 The plant nanofiltration unit (ZB – tank, ZO – drain valve, L – liquid level sensor, ZZ – check valve, PM – pump, F – flow meter, K – conductivity meter, ZR – regulation valve, ZOT – three-way valve, P – manometer, S – dry run sensor)

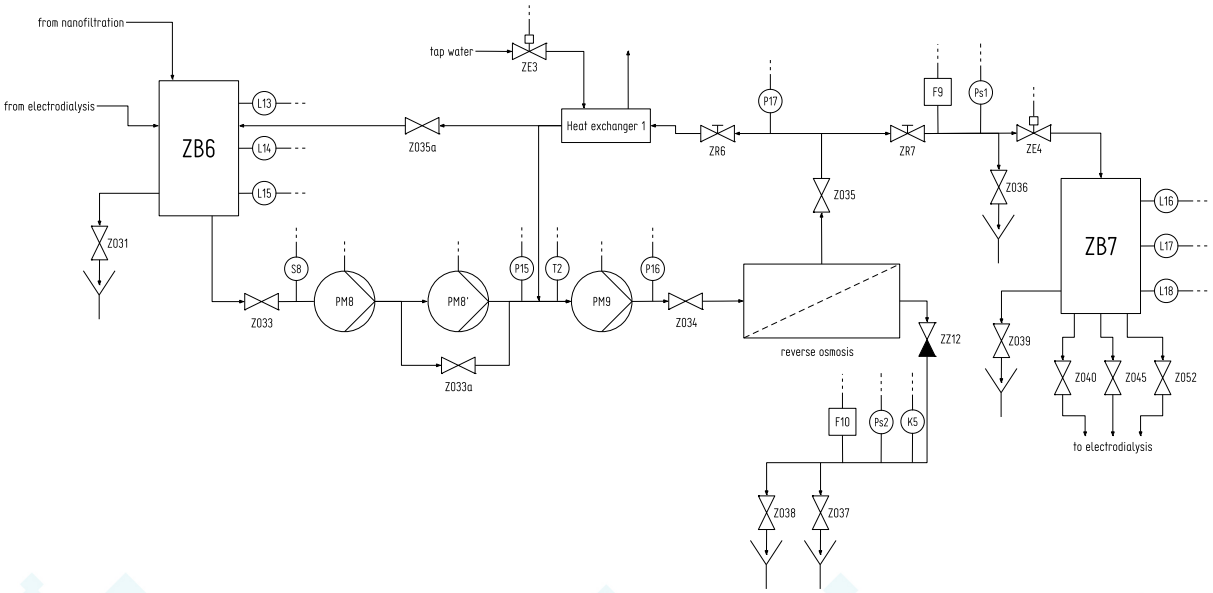

Figure 7 The plant reverse osmosis unit (ZB – tank, ZO – drain valve, ZE – electro-valve, S – dry run sensor, PM – pump, P – manometer, T – thermometer, L – liquid level sensor). The pipes leaving valves ZO40, ZO45, and ZO52 are connected to pipes entering valves ZO41, ZO46, and ZO53 in the electrodialysis unit, respectively

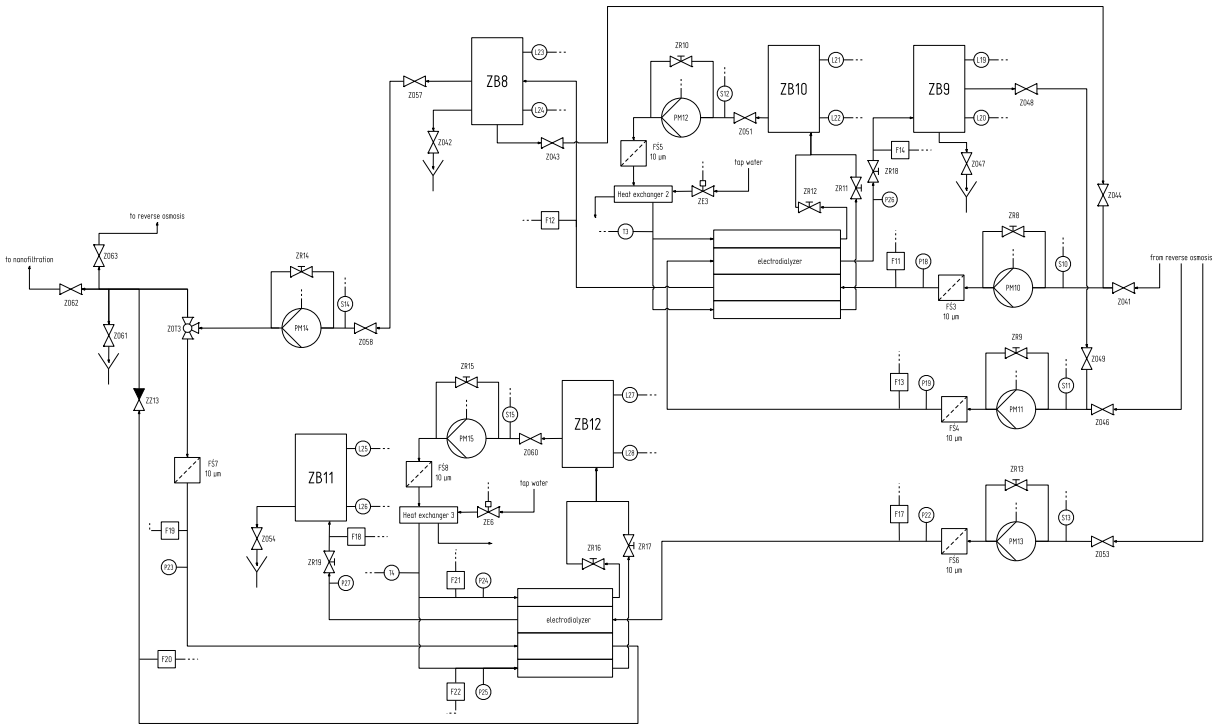

Figure 8 The plant electrodialysis unit (ZB – tank, FŚ – candle filter, PM – pump, F – flowmeter, P – manometer, T – thermometer, ZZ – check valve, ZO – drain valve, S – dry run sensor, L – liquid level sensor). The pipes entering valves ZO41, ZO46, and ZO53 are connected to the pipes leaving valves ZO40, ZO45, and ZO52 in the reverse osmosis unit, respectively

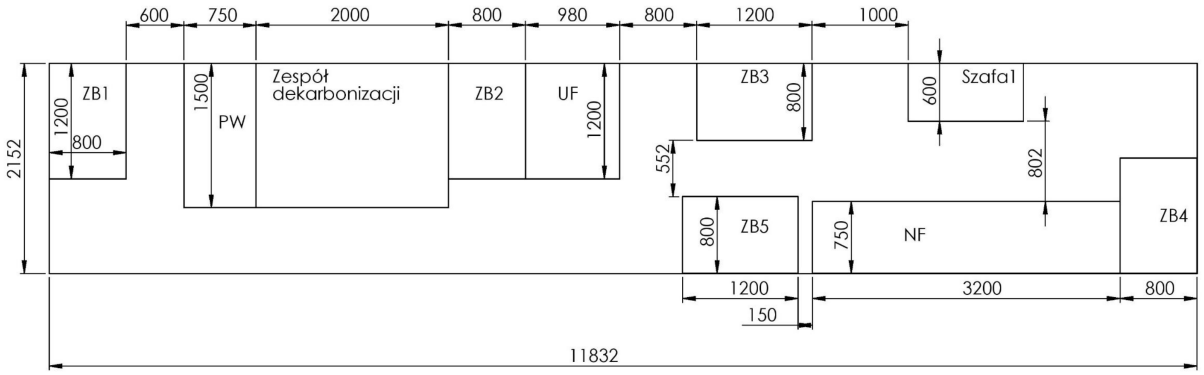

Figure 9 The location of plant units in the 1st container

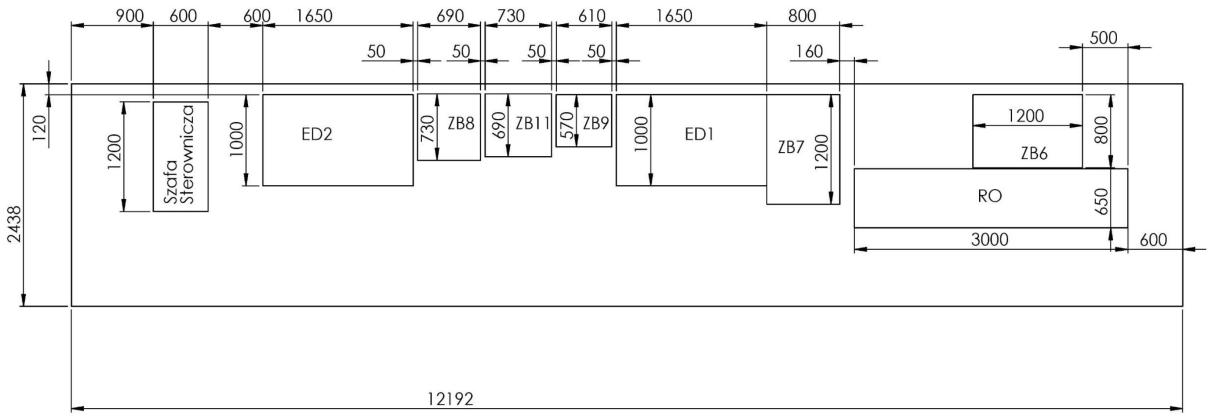

Figure 10 The location of plant units in the 2nd container

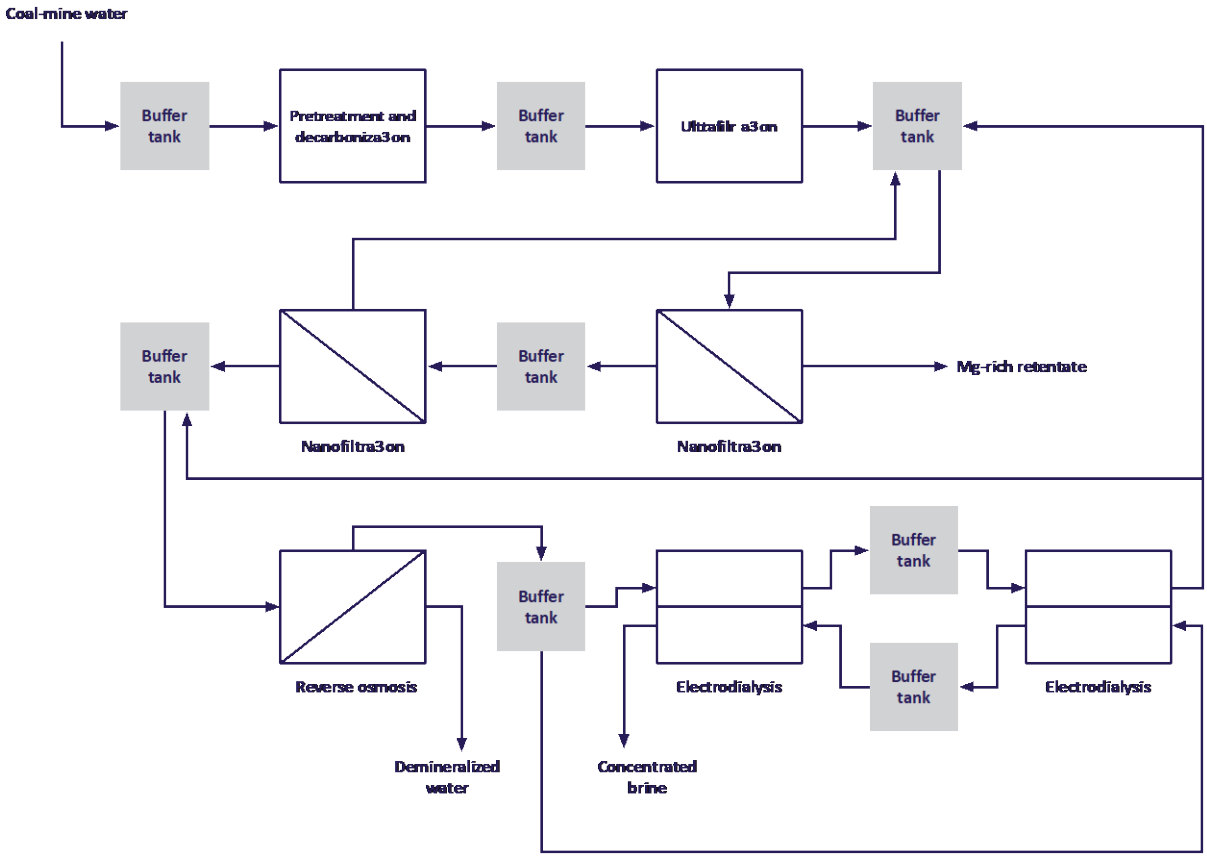

Figure 11 The general layout of the pilot plant – pretreatment (see Figure 3) and decarbonization (Figure 4), ultrafiltration (Figure 5), two-pass nanofiltration (Figure 6), reverse osmosis (Figure 7) and a cascade of two electrodialyzers (Figure 8)

3. Description of experiments performed during plant operation

a. Plant start-up

After the containers and the plant equipment (pretreatment, decarbonization, ultrafiltration, nanofiltration, reverse osmosis, electrodialysis) were delivered, assembled, tested for leaks, connections, sensors etc., it was discovered at the final day of the tests that the mine water is not available 24 h/day; in fact there are always irregular stops ranging from 3 to 5 h at the shift change. To accommodate that, the plant was stopped and the additional feed water buffer tanks were installed. The plant was then run for a 24 h/d, 7 days a week test, which lasted for two weeks (see Table 2 for the ionic composition of the samples collected during the plant run. Sampling points are depicted in Figure 12). A high consumption of pre-treatment filters was noted (see Table 2). The feed water (raw coal mine water) conductivity was highly variable, as depicted in Figure 13. Additionally, the decarbonization unit stopped working almost immediately, which was indicated by lack of pH decrease after the ion-exchange columns (the columns were regenerated on daily basis during the run, but the performance has not improved).

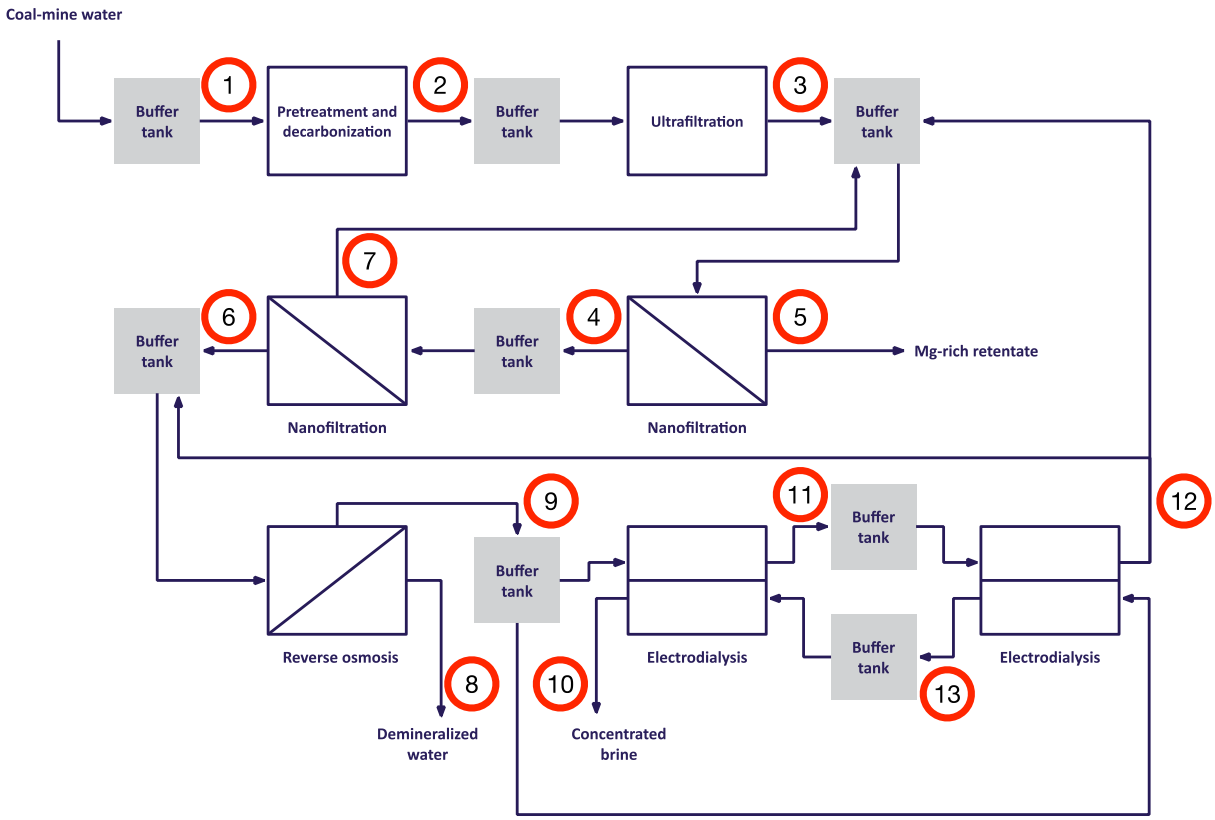

Figure 12 Sampling points for the plant process streams: 1) raw coal mine water, 2) feed after pretreatment and decarbonization, 3) ultrafiltration permeate, 4) 1st pass nanofiltration permeate, 5) 1st pass nanofiltration retentate, 6) 2nd pass nanofiltration permeate, 7) 2nd pass nanofiltration retentate, 8) reverse osmosis permeate, 9) reverse osmosis retentate, 10) 1st stage electrodialysis concentrate, 11) 1st stage electrodialysis diluate, 12) 2nd stage electrodialysis diluate, 13) 2nd stage electrodialysis concentrate

Table 2 Ionic composition of the samples collected during the plant start-up (see Figure 12)

	Sampling point	Ionic composition					
		Na^+, mg/L	Cl^-, mg/L	K^+, mg/L	Mg^{2+}, mg/L	Ca^{2+}, mg/L	SO_4^{2-}, mg/L
15	After pretreatment and decarbonization (2)	8890	15100	133	287	297	779
15	Ultrafiltration permeate (3)	8030	13500	118	248	263	621
15	1st pass nanofiltration permeate (4)	8560	14100	133	13	36	64
15	1st pass nanofiltration retentate (5)	10400	18100	154	405	440	1010
15	Reverse osmosis retentate (9)	9220	14600	141	<10	<10	41
15	1st stage electrodialysis diluate (11)	6310	10200	71	<10	<10	33
15	1st stage electrodialysis concentrate (10)	17800	28700	333	<10	12	61
16	Reverse osmosis permeate (8)	750	1300	13	<1	<1	2
20	After pretreatment and decarbonization (2)	2260	4950	53	238	546	713
20	Ultrafiltration permeate (3)	2840	5800	59	214	430	571
20	1st pass nanofiltration permeate (4)	2790	4790	60	11	59	27
20	1st pass nanofiltration retentate (5)	3590	7840	71	434	830	1170
20	2nd pass nanofiltration permeate (6)	3750	6210	67	<10	<10	<10
20	Reverse osmosis permeate (8)	57	119	1	<1	<1	<1
20	Reverse osmosis retentate (9)	6890	11000	113	<10	<10	10
20	1st stage electrodialysis diluate (11)	5440	8830	62	<10	<10	15
20	1st stage electrodialysis concentrate (10)	14000	22500	255	<10	12	26
21	1st pass nanofiltration permeate (4)	2790	4790	60	11	59	27
21	2nd pass nanofiltration permeate (6)	3750	6210	67	<10	<10	<10
63	Ultrafiltration permeate (3)	7670	13300	113	264	328	570
63	1st pass nanofiltration permeate (4)	7080	12500	108	205	285	54
63	2nd pass nanofiltration permeate (5)	6180	10500	100	66	156	<10
63	Reverse osmosis retentate (9)	8840	14400	122	86	191	<10
63	1st stage electrodialysis diluate (11)	6410	10500	72	46	86	<10
63	2nd stage electrodialysis diluate (12)	3760	5990	28	13	17	<10
63	1st stage electrodialysis concentrate (10)	12100	20400	197	141	352	<10
63	2nd stage electrodialysis concentrate (13)	13300	22100	203	141	320	22
64	1st pass nanofiltration retentate (5)	7410	12700	125	379	428	1220
66	1st stage electrodialysis diluate (11)	5550	9020	58	35	60	<10
66	2nd stage electrodialysis diluate (12)	3250	5230	22	<10	11	<10
66	1st stage electrodialysis concentrate (10)	16900	28400	278	199	483	<10
66	2nd stage electrodialysis concentrate (13)	12800	21300	185	126	267	<10
112	After pretreatment and decarbonization (2)	8100	13600	119	247	293	710
112	Raw coal mine water (1)	7980	13400	118	264	330	700
112	Ultrafiltration permeate (3)	7820	13400	117	245	295	699
112	1st pass nanofiltration permeate (4)	7300	12900	112	223	293	63
112	1st pass nanofiltration retentate (5)	8480	14800	127	404	433	1100
112	2nd pass nanofiltration permeate (6)	6150	10500	103	64	149	<10
112	Reverse osmosis retentate (9)	8730	14400	111	67	148	<10
112	1st stage electrodialysis diluate (11)	5960	9750	64	33	59	<10
112	2nd stage electrodialysis diluate (12)	3490	5650	24	<10	10	<10
112	1st stage electrodialysis concentrate (10)	16600	27600	258	167	430	11
112	2nd stage electrodialysis concentrate (13)	13200	21900	178	109	243	10
251	Reverse osmosis retentate (9)	9720	16100	122	107	182	16
251	1st stage electrodialysis diluate (11)	8370	13600	92	73	103	17
251	2nd stage electrodialysis diluate (12)	5970	9484	49	30	31	19
251	1st stage electrodialysis concentrate (10)	16400	27600	249	232	436	27
251	2nd stage electrodialysis concentrate (13)	13800	23100	193	175	298	24
256	Reverse osmosis permeate (8)	133	210	1	<1	<1	1
256	Reverse osmosis retentate (9)	9580	15900	120	105	184	28
262	After pretreatment and decarbonization (2)	7860	13600	120	288	441	750
262	Raw coal mine water (1)	4680	8500	83	238	470	714
285	1st pass nanofiltration permeate (4)	5560	10200	91	208	519	93
285	1st pass nanofiltration retentate (5)	6810	12100	105	410	815	1790
285	Reverse osmosis retentate (9)	9320	15300	114	91	259	22
285	1st stage electrodialysis diluate (11)	8100	13200	92	67	161	22
285	2nd stage electrodialysis diluate (12)	14100	23500	204	176	495	33
285	1st stage electrodialysis concentrate (10)	16600	28600	276	256	802	61
285	2nd stage electrodialysis concentrate (13)	6110	10100	58	35	63	23

Table 3 The filter replacements during the initial plant run (C – cleaning, R – replacement)

Date and time	Filter				
	FD1	FŚ1	FŚ1'	FŚ2	FM
12.07, 3:00		Replacement (20 µm)	Replacement (20 µm)	Replacement (20 µm)	Cleaning
12.07, 21:00		Replacement (20 µm)	Replacement (20 µm)		
13.07, 7:30	Cleaning	Replacement (20 µm)			
13.07, 9:30			Replacement (20 µm)		
13.07, 12:00					Replacement (20 µm)
13.07, 14:00				Replacement (20 µm)	
13.07, 18:20		Replacement (20 µm)			
15.07, 6:15				Replacement (20 µm)	
15.07, 9:00					Replacement (10 µm)
15.07, 14:30				Replacement (20 µm)	
16.07, 0:30				Replacement (20 µm)	
16.07, 8:20				Replacement (10 µm)	
16.07, 12:20		Replacement (20 µm)		Replacement (10 µm)	
16.07, 15:15			Replacement (20 µm)		
16.07, 17:10		Replacement (20 µm)	Replacement (20 µm)		
16.07, 21:00	Cleaning				
17.07, 5:30		Replacement (10 µm)			
17.07, 8:15		Replacement (20 µm)			
17.07, 12:00		Replacement (20 µm)	Replacement (20 µm)		
17.07, 13:00					Replacement (25 µm)
17.07, 17:40				Replacement (5 µm)	
18.07, 9:10		Replacement (20 µm)	Replacement (20 µm)		
18.07, 14:07		Replacement (20 µm)			
18.07, 19:20	Cleaning				
19.07, 23:00		Replacement (20 µm)	Replacement (20 µm)		
20.07, 1:00		Replacement (20 µm)	Replacement (20 µm)		
20.07, 3:00		Replacement (20 µm)	Replacement (20 µm)		
20.07, 10:25		Replacement (20 µm)	Replacement (20 µm)		
22.07, 2:45	Cleaning				
22.07, 13:10			Replacement (20 µm)		
22.07, 16:00		Replacement (20 µm)	Replacement (20 µm)		
22.07, 19:00		Replacement (20 µm)			

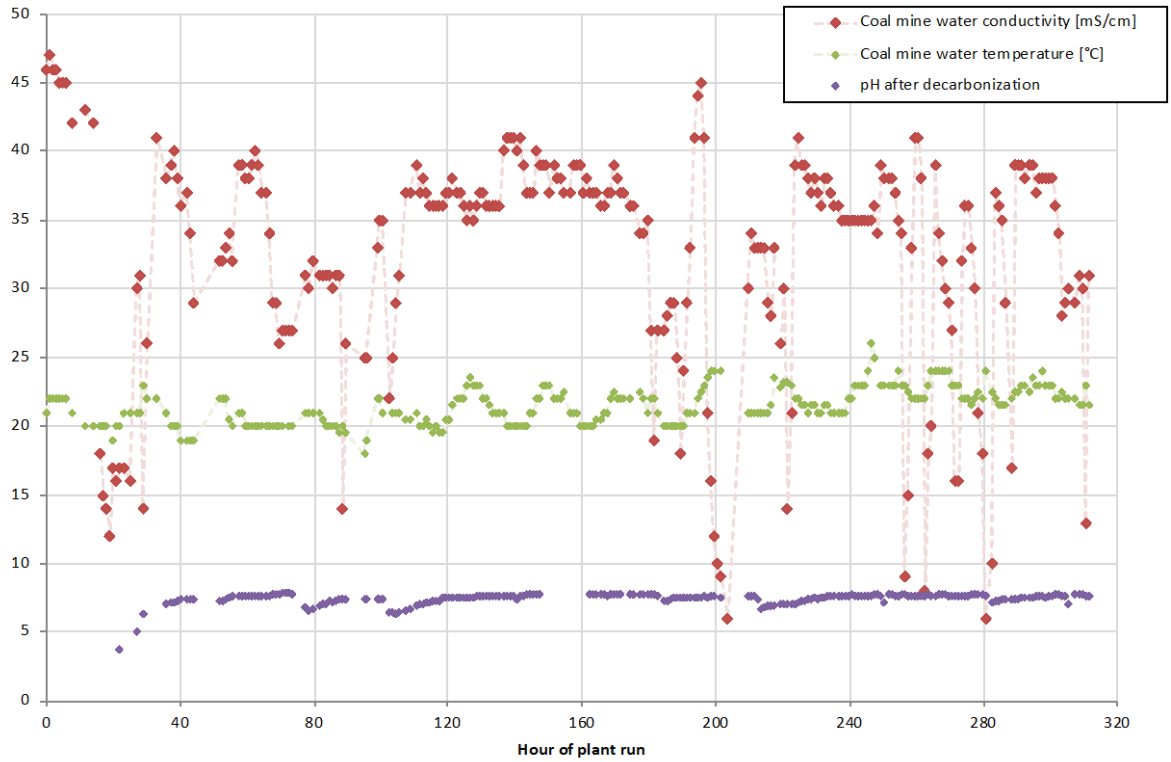

Figure 13 The coal mine water parameters and the performance of the decarbonization unit during the initial plant run

The ultrafiltration was working without major problems, although the capacity was too high for continuous work (see Figure 14) – this was addressed during subsequent modifications explained in Section 3b, "Modifications performed after initial run".

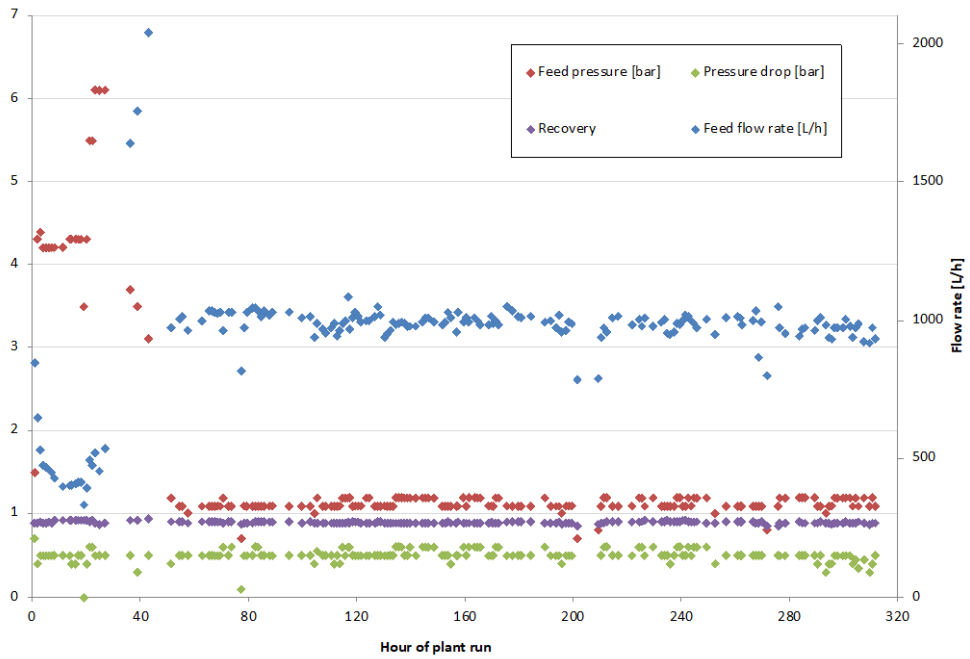

Figure 14 The performance of ultrafiltration during the initial plant run

Preliminary tests of nanofiltration were performed during the initial plant run (see Figures 15 and 16): for the first 18 h, the recovery of first-pass nanofiltration was set to 50%, then it was increased to 60% and eventually reached 70% at the 121 h of plant run. The first-pass retentate was discharged. No significant increase in hydraulic pressure drop, which would indicate the occurrence of scaling, was observed throughout the run. The second pass was working with recovery ca. 55%, but since all the of second-pass retentate was recycled to the first-pass nanofiltration, increasing the recovery was not worth the risk of membrane scaling.

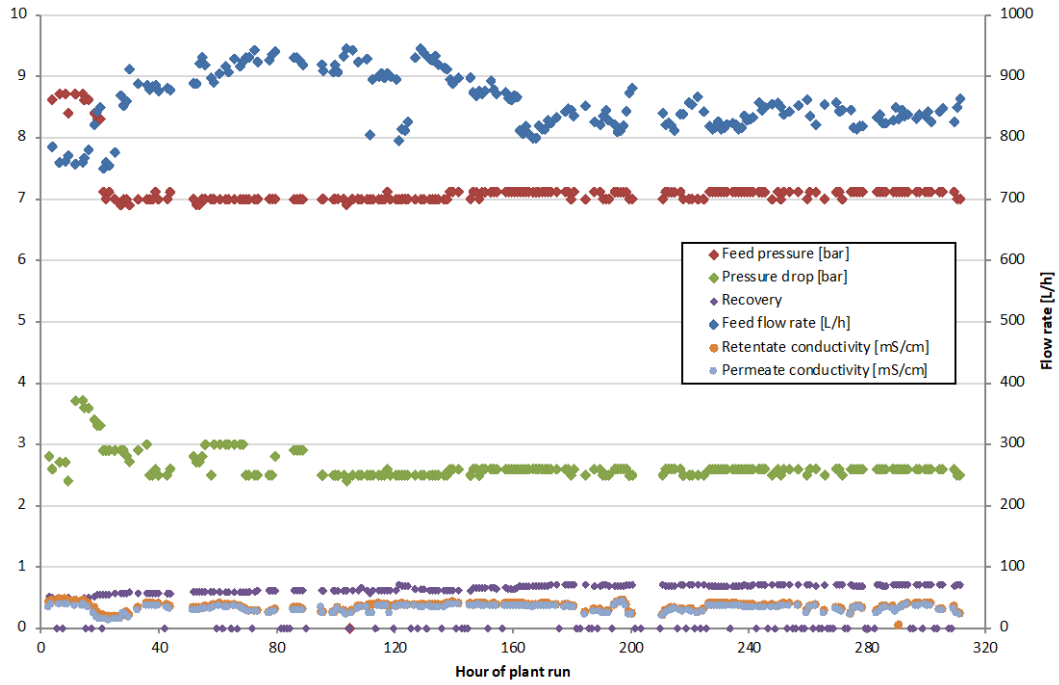

Figure 15 The performance of first-pass nanofiltration during the initial plant run

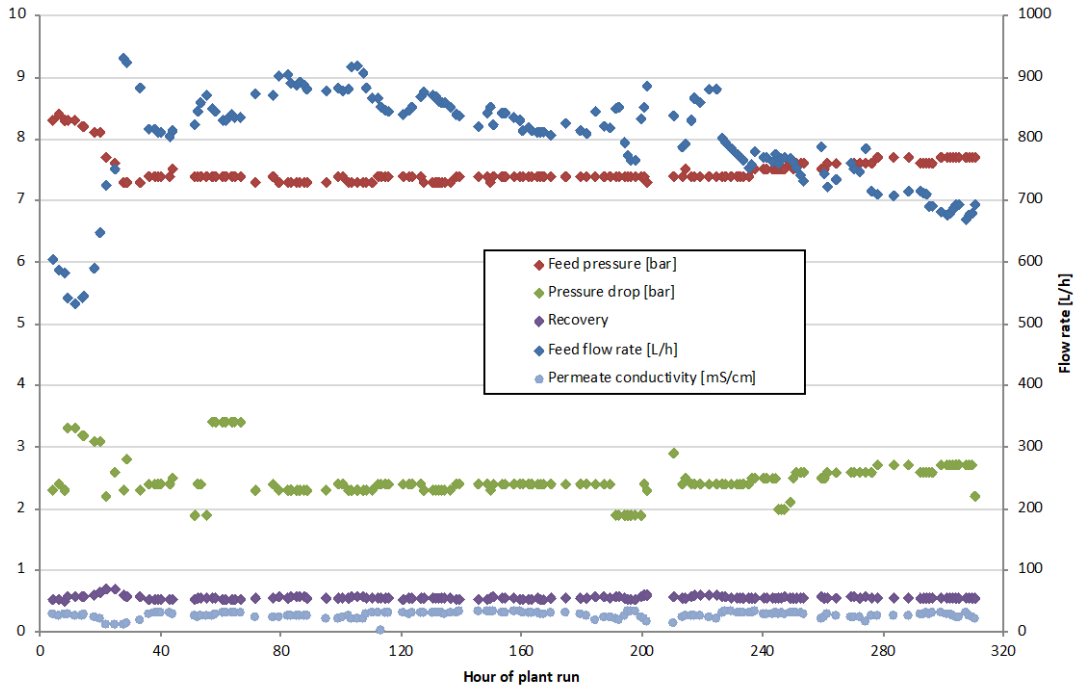

Figure 16 The performance of second-pass nanofiltration during the initial plant run

Reverse osmosis unit also did not experience problems (see Figure 17), expect for too high capacity, which was addressed during the subsequent modifications.

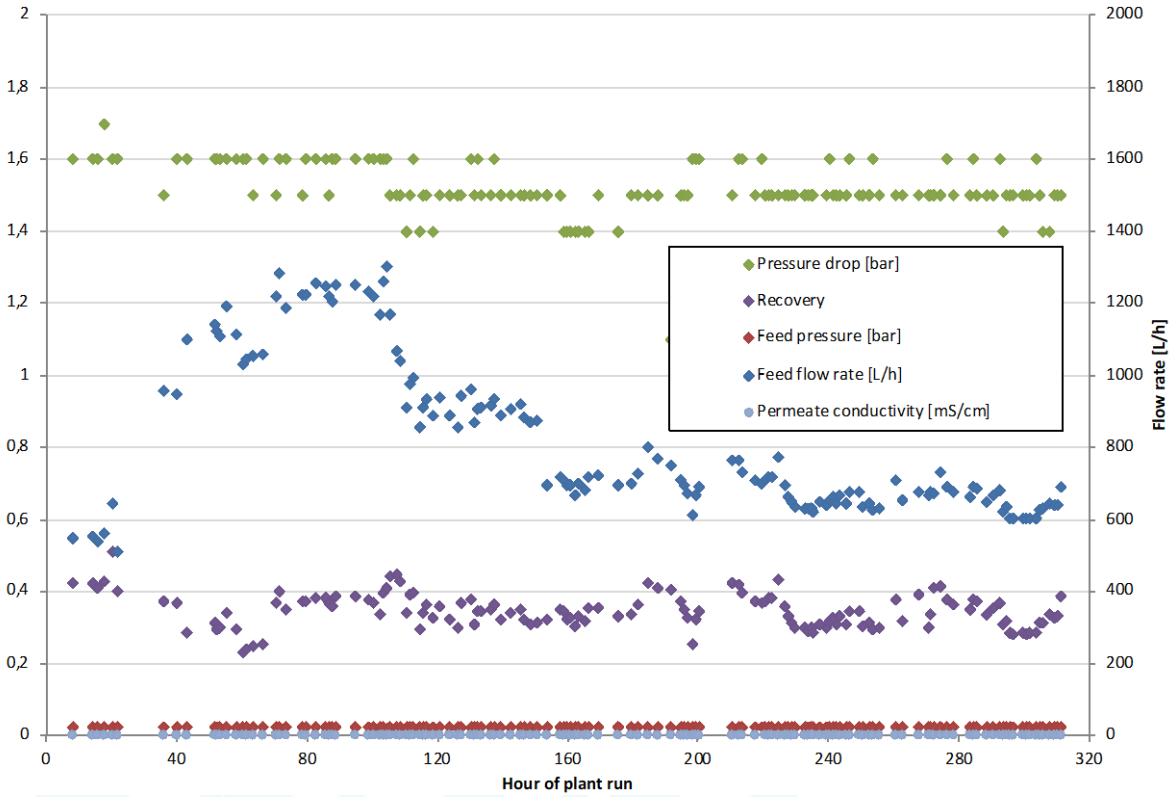

Figure 17 The performance of reverse osmosis during the initial plant run

Due to the pump malfunction, the second stage of electrodialysis was started after 36 h of plant run. After that, both first and second stages worked as a counter-current cascade, i.e. the reverse osmosis retentate was pumped through first-stage ED diluate chamber, where it was preliminarily desalted, and then was pumped through second-stage ED diluate chamber for deeper desalination. The obtained diluate was recycled back to first-pass nanofiltration. On the other side of the cascade, the reverse osmosis retentate was first pumped through the concentrate chamber of second-stage ED, where it was preliminarily concentrated, and then was pumped through first-stage ED concentrate chamber for further concentration.

The electrodialyzers worked in the constant-voltage mode. A decrease in current over time was observed (see Figures 18 and 19), which indicate scaling increasing the overall stack electric resistance. This was confirmed after disassembling the module – a white solid was deposited on the ion-exchange surface. This can be contributed to the malfunctioning decarbonization unit – the bicarbonate ions present in coal mine water, not removed by ultrafiltration and nanofiltration, were concentrated by reverse osmosis, which created a scaling conditions inside the electrodialyzer working on reverse osmosis retentate.

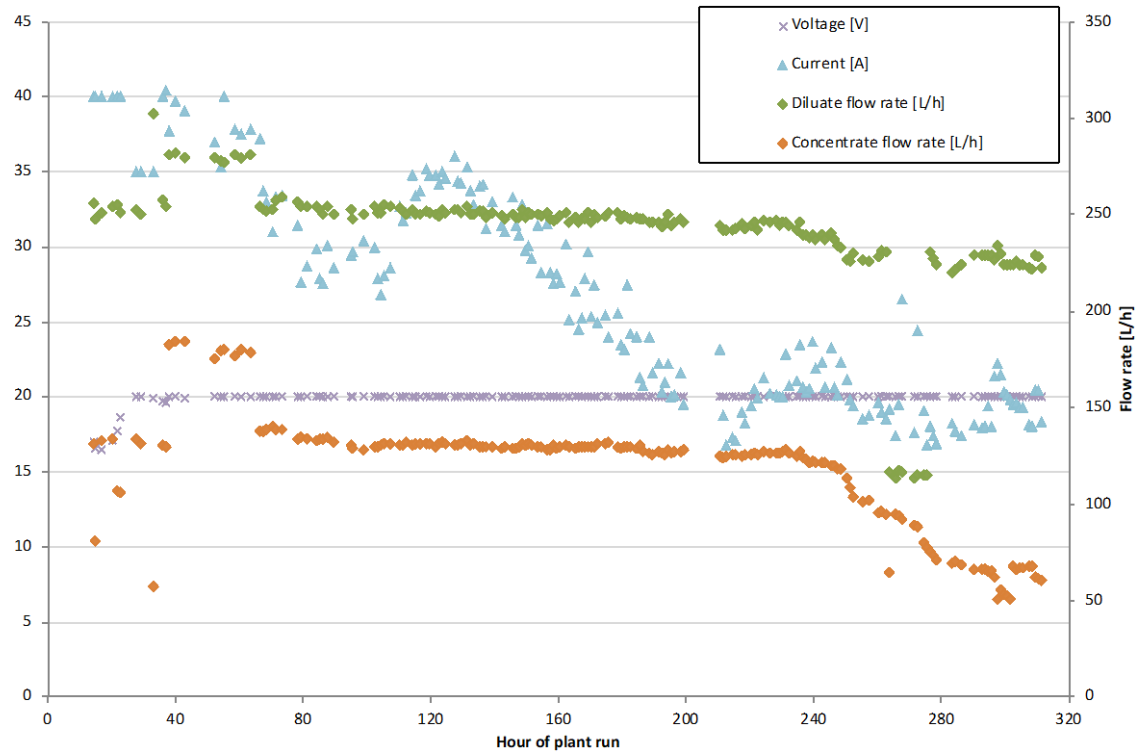

Figure 18 The performance of first-stage electrodialyzer during the initial plant run

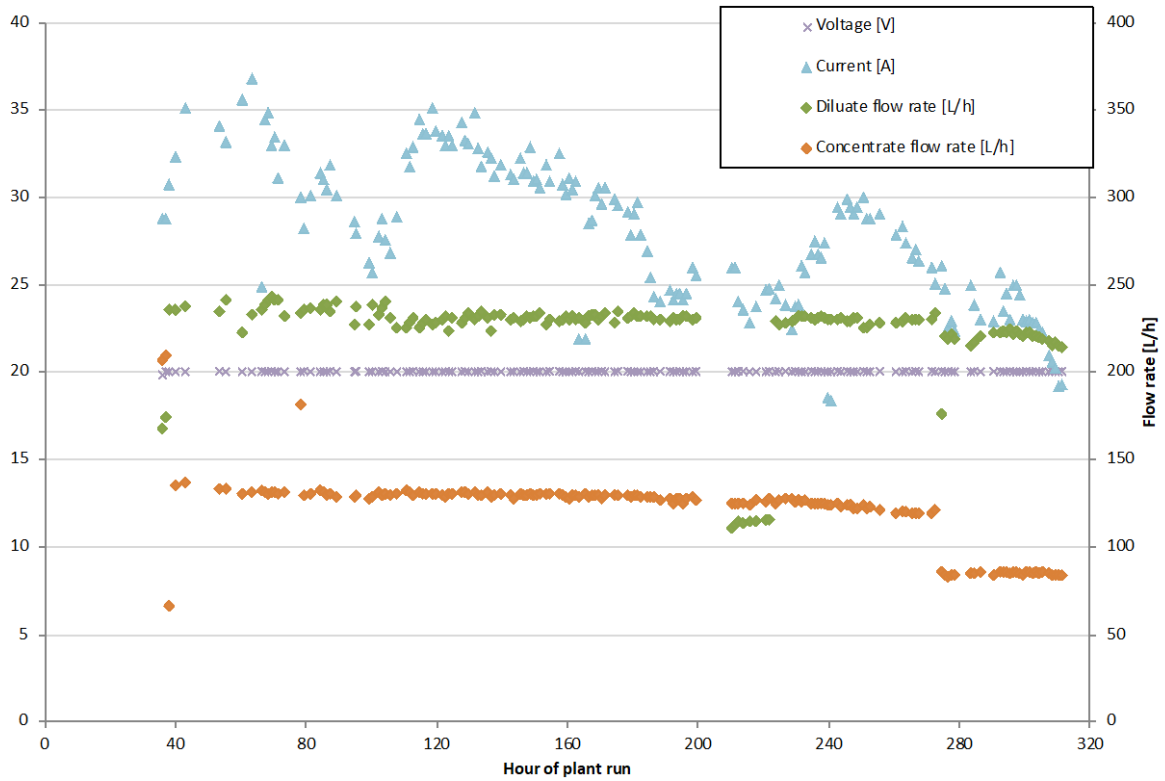

Figure 19 The performance of first-stage electrodialyzer during the initial plant run

b. Modifications performed after initial run

During the initial pilot plant run, several problems appeared and were solved as follows:

- The water supply was not, as previously expected, continuous. In fact, the feed flow interruptions usually took several hours a day – this was accommodated by installing additional buffer tanks, so that the excess of coal mine water can be collected. The additional buffer tanks fixed the issue and the continuous operation was possible after the modification.
- The raw coal mine water contained a lot more carbon suspension than previously anticipated. During the initial sampling, the mine water was clear and devoid of suspended particles. The water fed to the pilot plant was black and had a high number of suspended particles, which tend to block the 10, 25, 50 and 200 µm cartridge filters very quickly. It's unclear whether something changed in the mine dewatering system during or the samples of coal mine water provided by the PGG (see Deliverable 3.1) were collected from the settler and not directly from the dewatering system. To mitigate the problem with carbon suspension, following modifications were committed: 1) replace initial slit filter FD1 with automatic self-cleaning filter in order to avoid constant need of supervision and manual cleaning, 2) move the feed inlet pipe to a different buffer tank than the plant intake pipe, so that the first buffer tank can act as settler. The addition of a 1 m^3 buffer tank working as settler fixed the problems and no downtime caused by pretreatment filters clogging up.
- The decarbonization unit broke down almost immediately. After about 20 h of constant operation the pH after decarbonization raise from below 4 to about 7-7.5 – the same as the pH of raw coal mine water. The ion-exchange column used for the decarbonization was clogged with the very small particles (< 1 µm) of suspended carbon. To mitigate the problem, the decarbonization unit was moved to work on the

ultrafiltration permeate. After washing and cleaning the decarbonization unit, the problems did not reappear when working on the UF permeate.

- The capacity of UF, NF, RO was too high, which caused frequent stops due to lack of feed water and prevented continuous operation. This was mitigated by implementing pump bypasses.
- After the modifications were complete, a severe problem with air in the feed water inlet started to occur. The build-up of air the automatic self-cleaning filter prevented both continuous operation and filling up the feed buffer tanks in reasonable time. The filter basically required manual disassembly and reassembly every 5 h, so the operation was stopped completely. During the downtime, ion-exchange columns were cleaned, the filling rings in the degassing column were dismounted, cleaned and remounted, the self-cleaning filter was modified to allow automatic evacuation of build-up air. The coal mine also installed de-airing on the connection to the dewatering system, but the results were not satisfactory. Eventually the problems were fixed by significantly increasing the plant inflow and retrofitting the buffer tanks with overspill collectors which recycled the feed water back to the mine watering system. In that way the liquid level in the feed buffer tanks was kept high when there was no air in the dewatering system, so there was enough water to work on when the gas started to appear again.
- A thermal insulation was installed on the tap water pipeline (tap water is used in heat exchangers and for flushing the ion-exchange columns after regeneration), as it had frozen during the night downtime in the below zero temperatures experienced at the site between October and March. This problem was not completely fixed and caused few downtimes; however, they were not frequent enough to prevent all planned experiments.

c. Maximum safe recovery in nanofiltration

Recovery in nanofiltration is limited by the risk of sparingly soluble salts crystallization in the retentate - it would result in clogging the membrane modules and their malfunction. In order to assess the maximum permissible recovery, the retentate has been gradually chocked in the first-pass nanofiltration (NF1) and the hydraulic pressure drop (i.e. the difference between retentate and feed) has been monitored. The sudden increase in this value would indicate blocking the module by the deposits. The recovery in the second-pass nanofiltration (NF2) was 80%. The recovery of 60, 70, and 80% has been studied in the first pass, more endangered for sparingly soluble salts crystallization. No significant change in hydraulic pressure drop has been observed for the tested recovery (Figure 20). Work at higher recovery would be too risky because of existing supersaturation of calcium sulphate in the retentate - at 80% recovery the retentate was already supersaturated, but because of slow crystallization kinetics, it only precipitated in the collected retentate samples after few hours. Because the hydraulic residence time in NF module is lower than the time required for observing the macroscopic crystallization, it can be concluded that work at 80% recovery in first-pass nanofiltration is safe in continuous mode. It was unwittingly confirmed during system malfunction, which forced 2 h shutdown when the module was already working at 80% recovery. After removing the malfunction and restarting the NF1, no significant change in module operation was observed.

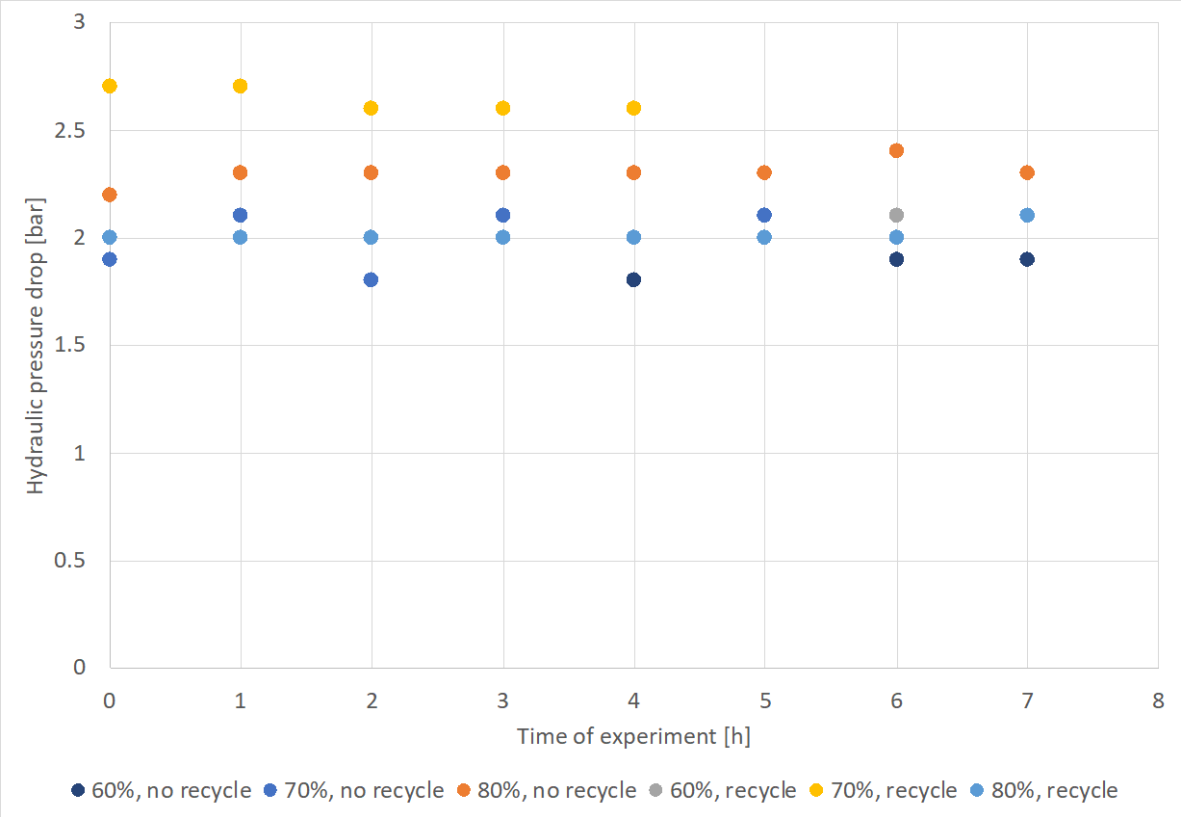

Figure 20 The influence of NF recovery on the NF1 hydraulic pressure drop during the tests

Table 4 presents the composition of raw water, permeate and retentate. The results show good separation between univalent and bivalent ions, which indicates the possibility of magnesium hydroxide recovery from the retentate stream with simultaneous salt recovery from the permeate stream.

Table 4 Dependence of ionic composition of streams leaving the double-pass nanofiltration on first-pass permeate recovery and second-pass recycle (NF2 recovery = 80%)

		Recovery in first-pass nanofiltration					
		NF2 retentate recycled			NF2 retentate not recycled		
		60%	70%	80%	60%	70%	80%
Feed water [mg/dm³]	Cl^-	13 200	13 432	14 000	13 200	13 400	12 700
	SO_4^{2-}	638	647	618	638	656	622
	Na^+	7 920	8 164	8 400	7 920	7 980	7 670
	K^+	122	126	118	122	123	111
	Mg^{2+}	228	279	246	228	276	247
	Ca^{2+}	231	306	289	231	334	290
NF 1 retentate [mg/dm³]	Cl^-	15 800	17 454	21 200	15 700	17 000	17 100
	SO_4^{2-}	1 810	1 643	2 770	1 430	2130	2 920
	Na^+	8 840	9 837	11 000	9 030	9 340	8 890
	K^+	130	148	133	137	140	123
	Mg^{2+}	655	697	1 100	503	802	1 070
	Ca^{2+}	613	769	1 200	493	719	983
NF2 permeate [mg/dm³]	Cl^-	10 100	12 543	11 100	10 500	12 200	12 200
	SO_4^{2-}	< 10	< 10	12	< 10	18	17
	Na^+	6 320	8020	7 010	6 610	7 600	7 560
	K^+	100	121	103	104	118	104
	Mg^{2+}	< 10	4	< 10	< 10	12	< 10
	Ca^{2+}	< 10	33	<10	14	25	28

The two-pass nanofiltration system has shown very high rejection coefficients (see Table 5) with respect two bivalent ions and relatively low rejection coefficients of univalent ions, which is a desired behaviour from the point of view of separating sodium chloride from calcium and magnesium.

Table 5 Rejection of ions in the two-pass nanofiltration system

		Recovery in first-pass nanofiltration					
		NF2 retentate recycled			NF2 retentate not recycled		
		60%	70%	80%	60%	70%	80%
Rejection [%]	Cl^-	23.5%	6.6%	20.7%	20.5%	9.0%	3.9%
	SO_4^{2-}	98.4%	98.5%	98.1%	98.4%	97.3%	97.3%
	Na^+	20.2%	1.8%	16.5%	16.5%	4.8%	1.4%
	K^+	18.0%	4.0%	12.7%	14.8%	4.1%	6.3%
	Mg^{2+}	95.6%	98.6%	95.9%	95.6%	95.7%	96.0%
	Ca^{2+}	95.7%	89.2%	96.5%	93.9%	92.5%	90.3%

d. Single-pass electrodialysis

The experiments were conducted in the cascade of two electrodialyzers working in the single-pass mode. The feed was the reverse osmosis retentate working on the nanofiltration permeate (NF1 recovery 80%, NF2 recovery 80%, NF2 retentate completely recycled before NF2). The current density in both electrodialyzers was kept constant. Two PC-Cell 1000 A modules were used, each equipped with 25 pairs of IONSEP K/A membranes separated with 0.35 mm spacers. The volumetric flow rate was 8 dm^3/h in the concentrate chamber and 119 dm^3/h in the diluate chamber. The composition of the obtained concentrates is presented in Tables 6-10. The obtained brine has relatively low concentration of bivalent contaminants (SO_4^{2-}, Mg^{2+}, Ca^{2+}), which indicates reaching higher salt recovery in case of brine use in evaporated salt production, and stems from the application of nanofiltration before the reverse osmosis; the brine is not sufficiently saline, however, to be directly fed to the crystallizer and requires further concentration. This indicates the necessity of further optimization of electrodialysis, in particular the second step of the cascade, in which the increase in concentration is lower than in the first step of the cascade. It may be a result of the application of different membranes - the differences in chemical composition of the membrane may cause the differences in ions and water transport, affecting the obtained concentrate. Figure 21 presents the voltage drop per membrane pair (each electrodialyzer consisted of 25 membrane pairs). Higher voltage drop could be dangerous to the membranes and indicate overcoming the limiting current density, but during the experiments voltage drop higher than 1.2 V/cell pair (which is the standard potential of water splitting reaction occurring when the current density is higher than limiting current density) was observed only at highest current density with the electrodialyzer ED2, which produces the least concentrated diluate. Figure 22 presents the energy consumption in the electrodialysis. Because high current density was applied, the energy consumption in relatively high, which also indicates the necessity of further optimization. On the other hand, if the proposed technology is to implemented where there is waste heat available, further concentration by electrodialysis may not be required - instead an efficient thermal method may be cheaper. Such solution is however beyond the scope of the tests in this pilot plant and strongly depends on the situation in the specific mine.

Table 6 Composition of solutions obtained during single-pass electrodialysis tests, current density 390 A/m^2

Stream		Reverse osmosis retentate	Concentrate after 1st stage of ED cascade	Concentrate after 2nd stage of ED cascade
Concentration [mg/dm^3]	Cl^-	25 300	51 700	65 400
	SO_4^{2-}	10	25	145
	Na^+	16 000	32 400	41 000
	K^+	239	505	775
	Mg^{2+}	20	47	57
	Ca^{2+}	102	240	414

Table 7 Composition of solutions obtained during single-pass electrodialysis tests, current density 455 A/m^2

Stream		Reverse osmosis retentate	Concentrate after 1st stage of ED cascade	Concentrate after 2nd stage of ED cascade
Concentration [mg/dm^3]	Cl^-	26 100	57 600	83 500
	SO_4^{2-}	21	70	240
	Na^+	19 000	42 300	61 700
	K^+	285	590	1170
	Mg^{2+}	18	41	73
	Ca^{2+}	98	198	477

Table 8 Composition of solutions obtained during single-pass electrodialysis tests, current density 519 A/m^2

Stream		Reverse osmosis retentate	Concentrate after 1st stage of ED cascade	Concentrate after 2nd stage of ED cascade
Concentration [mg/dm^3]	Cl^-	25 100	64 400	60 400
	SO_4^{2-}	10	77	109
	Na^+	15 900	40 500	37 800
	K^+	246	572	717
	Mg^{2+}	23	54	54
	Ca^{2+}	115	246	394

Table 9 Composition of solutions obtained during single-pass electrodialysis tests, current density 584 A/m^2

Stream		Reverse osmosis retentate	Concentrate after 1st stage of ED cascade	Concentrate after 2nd stage of ED cascade
Concentration [mg/dm^3]	Cl^-	25 400	66 400	83 700
	SO_4^{2-}	13	59	167
	Na^+	16 100	42 100	52 700
	K^+	238	552	1 010
	Mg^{2+}	18	39	46
	Ca^{2+}	94	202	445

Table 10 Composition of solutions obtained during single-pass electrodialysis tests, current density 649 A/m²

Stream		Reverse osmosis retentate	Concentrate after 1st stage of ED cascade	Concentrate after 2nd stage of ED cascade
Concentration [mg/dm³]	Cl^-	28 517	95 800	111 000
	SO_4^{2-}	102	727	621
	Na^+	18 165	59 600	68 700
	K^+	664	649	1 190
	Mg^{2+}	16	< 50	< 50
	Ca^{2+}	94	77	189

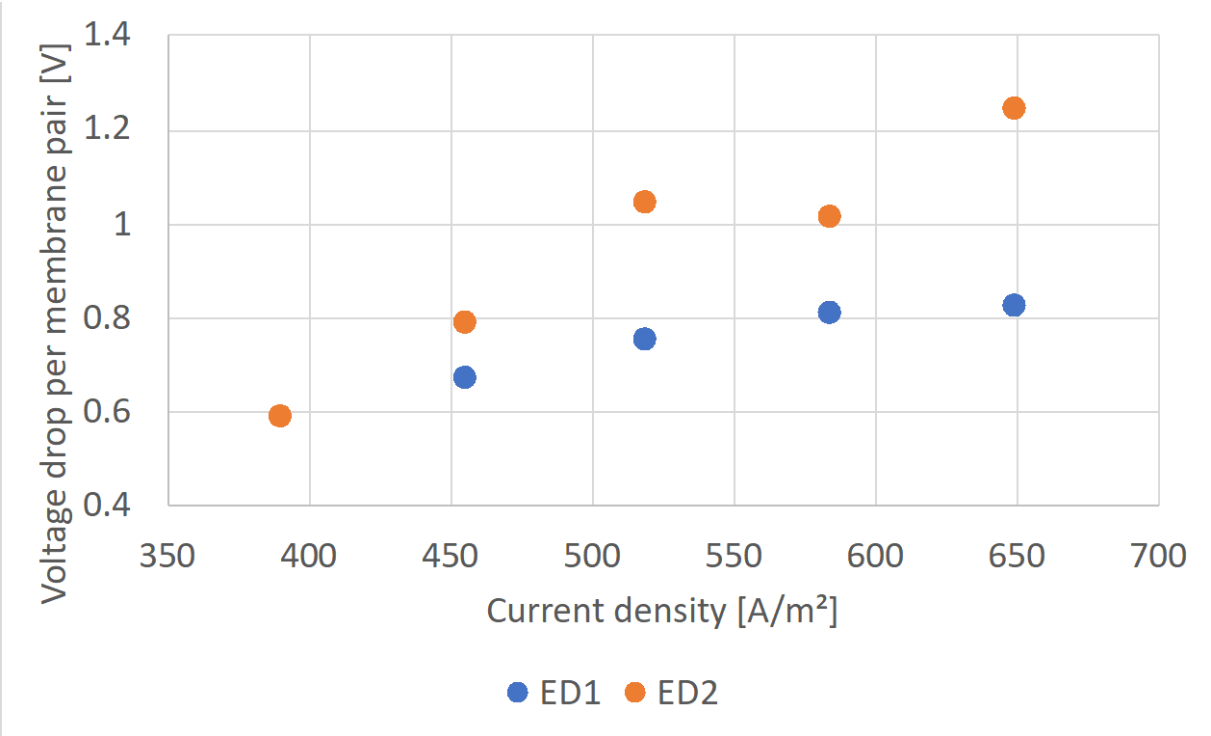

Figure 21 Voltage drop per membrane pair in the single-pass electrodialyzers

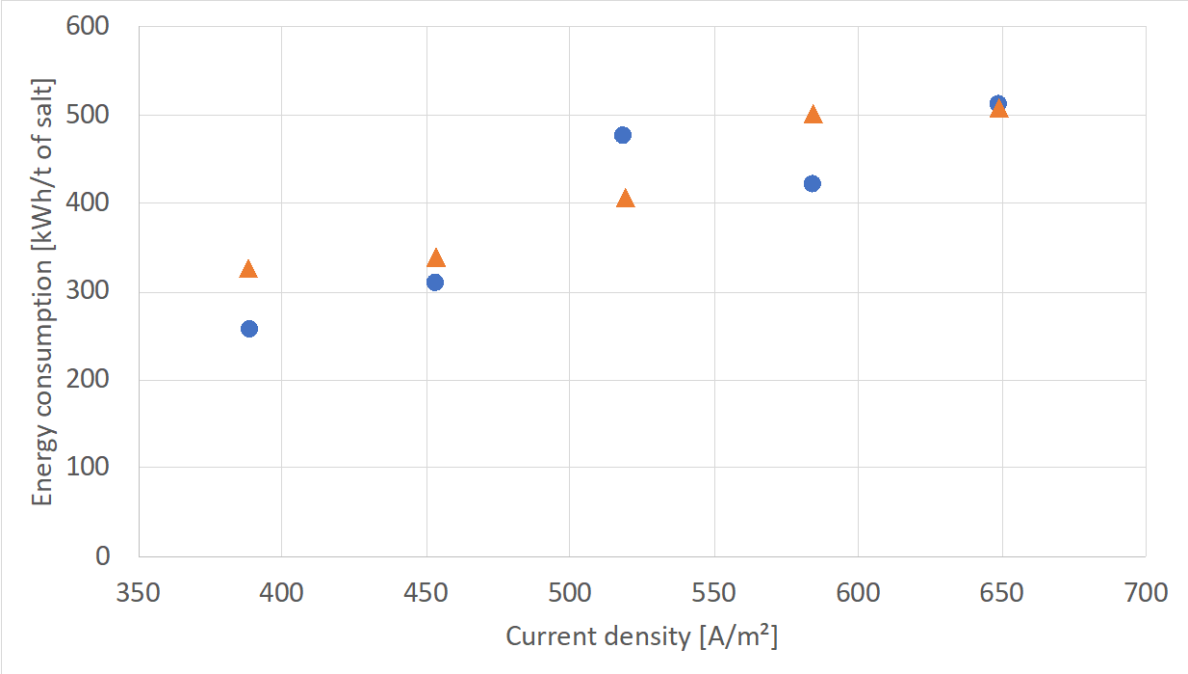

Figure 22 Dependence of DC energy consumption on the applied current density

e. Batch-mode electrodialysis

The experiments were conducted in a PC-Cell 1000 A electrodialyzer working in the batch mode, equipped with 25 pairs of IONSEP K/A membranes separated with 0.35 mm spacers. The results are presented in Tables 11-17. The influence of current density and diluate:concentrate initial volume ratio on the ion and water transport was investigated.

Table 11 The results of batch-mode electrodialysis, current density 649 A/m^2, diluate:concentrate initial volume ratio 7:1

Time [h]		0	0.25	0.5	0.75	1	1.25	1.5	1.75	2	2.25	2.5	2.75	3	3.25	3.5
Stack voltage drop [V]		26.9	25.6	25	24.5	24.3	25.2	24.7	24	24.7	24.4	24.4	24.2	24.7	31.1	35
Applied current [A]		50	50	50	50	50	50	50	50	50	50	50	50	50	50	48.2
Diluate inlet flow rate [L/h]		110	111	110	111	111	117	117	119	122	123	129	126	130	130	132
Diluate outlet flow rate [L/h]		100	104	104	104	105	109	111	113	118	116	117	118	122	123	124
Concentrate inlet flow rate [L/h]		75	94	97	99	100	103	106	108	109	111	111	117	115	119	121
Concentrate outlet flow rate [L/h]		86	103	104	108	109	112	116	116	119	121	122	124	127	128	130
Mean stack temperature [°C]		15	16	17	17	18	20	21	22	24	24	26	27	28	29	30
Diluate tank volume [L]		175	172	170	168	165	162	162	160	158	157	155	153	150	147	145
Concentrate tank volume [L]		25	27	30	31	33	35	36	37	40	41	42	44	47	47	50
Diluate composition[mg/dm^3]	**Cl^-**	30300			20080			10100			6040			5210		4180
	SO_4^{2-}	292			217			177			252			91		73
	Na^+	18100			12750			6460			3870			3360		2690
	K^+	272			80			56			136			32		31
	Mg^{2+}	27			< 10			< 10			17			< 10		< 10
	Ca^{2+}	94			24			15			46			< 10		< 10
Concentrate composition[mg/dm^3]	**Cl^-**	32300			65000			81200			88600			93100		93800
	SO_4^{2-}	159			377			546			712			962		1046
	Na^+	19300			38000			48500			52600			55600		55700
	K^+	294			709			842			864			845		829
	Mg^{2+}	28			57			72			80			82		81
	Ca^{2+}	102			247			300			309			297		290

Table 12 The results of batch-mode electrodialysis, current density 390 A/m^2, diluate:concentrate initial volume ratio 10:1

Time [h]		0	0.5	1	1.5	2	2.5	3	3.5	4	4.5	5	5.5	6	6.5	7	7.5	8	8.5	9
Stack voltage drop [V]		17.5	16.9	15.6	15.6	15.4	15.2	15.3	15.5	15.4	15.4	15.6	15.9	16.2	16.9	17.6	18.5	21.1	27.1	35
Applied current [A]		30	30	30	30	30	30	30	30	30	30	30	30	30	30	30	30	30	30	30
Diluate inlet flow rate [L/h]		106	104	106	109	109	112	112	114	117	118	119	119	120	120	122	122	123	124	125
Diluate outlet flow rate [L/h]		97	101	101	104	106	108	108	108	112	112	114	115	114	116	119	119	120	120	120
Concentrate inlet flow rate [L/h]		74	96	98	101	104	105	105	106	108	108	112	113	113	114	116	118	118	119	120
Concentrate outlet flow rate [L/h]		84	102	104	107	111	113	111	112	114	116	117	120	121	122	122	124	126	127	127
Mean stack temperature [°C]		13	15	16	18	19	21	22	23	24	25	26	27	28	28	29	30	31	32	33
Diluate tank volume [L]		190	188	185	183	181	179	177	175	171	170	168	164	161	160	158	157	152	151	150
Concentrate tank volume [L]		18	20	23	24	26	29	31	33	35	37	39	42	44	46	48	50	53	54	56
Diluate composition[mg/dm^3]	**Cl^-**	30450			20640			15980			11840			8860			6270			6320
	SO_4^{2-}	36			102			133			147			135			112			96
	Na^+	19420			13130			10200			7570			5710			4050			4070
	K^+	284			140			104			76			57			44			39
	Mg^{2+}	< 25			< 10			< 10			< 10			< 10			< 10			< 10
	Ca^{2+}	30			16			10			< 10			< 10			< 10			< 10
Concentrate composition[mg/dm^3]	**Cl^-**	30450			68790			81400			84920			85640			84320			83560
	SO_4^{2-}	36			36			589			783			971			1150			1500
	Na^+	19420			43660			49760			53780			54340			53810			53320
	K^+	284			286			827			915			917			869			774
	Mg^{2+}	< 25			< 25			< 25			< 25			< 25			< 25			< 25
	Ca^{2+}	30			31			108			125			127			118			100

Table 13 The results of batch-mode electrodialysis, current density 519 A/m^2, diluate:concentrate initial volume ratio 10:1

Time [h]		0	0.5	1	1.5	2	2.5	3	3.5	4	4.5	5	5.5	6	6.5
Stack voltage drop [V]		20.1	19.5	18.3	17.5	17.6	17.1	17.3	17.6	17.9	18.4	18.7	19.8	21	26
Applied current [A]		40	40	40	40	40	40	40	40	40	40	40	40	40	40
Diluate inlet flow rate [L/h]		98	102	103	105	106	106	107	108	108	109	109	111	110	112
Diluate outlet flow rate [L/h]		97	99	101	101	103	103	102	103	103	104	105	106	106	106
Concentrate inlet flow rate [L/h]		111	115	115	119	118	114	114	116	120	120	120	119	121	125
Concentrate outlet flow rate [L/h]		111	121	120	126	125	121	121	122	124	126	126	126	129	129
Mean stack temperature [°C]		18	22	23	24	25	25	26	28	28	30	31	31	32	33
Diluate tank volume [L]		190	187	185	184	181	179	178	175	172	169	168	165	162	160
Concentrate tank volume [L]		19	21	22	24	26	27	30	32	34	37	38	41	43	45
Diluate composition[mg/dm^3]	**Cl^-**	31600		18310		15380		15020		11600		9540		7920	6060
	SO_4^{2-}	87		137		151		169		163		150		134	115
	Na^+	18800		11690		9840		9580		7450		6150		5140	3940
	K^+	280		126		102		102		78		66		54	51
	Mg^{2+}	10		< 10		< 10		< 10		< 10		< 10		< 10	< 10
	Ca^{2+}	40		16		13		12		< 10		< 10		< 10	< 10
Concentrate composition[mg/dm^3]	**Cl^-**	31000		71400		86200		94200		97400		98300		98300	97900
	SO_4^{2-}	63		534		761		894		1053		1214		1402	1494
	Na^+	18500		42800		51500		55600		57100		57800		57800	57600
	K^+	281		772		914		960		958		933		897	864
	Mg^{2+}	10		< 25		29		< 50		< 50		< 50		< 50	< 50
	Ca^{2+}	38		115		139		147		153		147		133	125

Table 14 The results of batch-mode electrodialysis, current density 649 A/m^2, diluate:concentrate initial volume ratio 10:1

Time [h]		0	0.25	0.5	0.75	1	1.25	1.5	1.75	2	2.25	2.5	2.75	3	3.25	3.5	3.75	4
Stack voltage drop [V]		25.3	23.6	23	23	22.4	22.2	21.5	21.2	21.2	21.3	21.8	21.8	22.4	22.8	23.3	23.9	31.5
Applied current [A]		50	50	50	50	50	50	50	50	50	50	50	50	50	50	50	50	50
Diluate inlet flow rate [L/h]		111	116	116	116	118	118	120	121	123	112	113	114	115	116	117	115	118
Diluate outlet flow rate [L/h]		108	110	111	109	115	113	114	116	117	106	106	106	111	110	109	109	111
Concentrate inlet flow rate [L/h]		89	81	86	88	90	100	99	107	112	109	109	113	114	115	117	118	120
Concentrate outlet flow rate [L/h]		86	89	93	95	98	103	106	114	118	115	119	120	122	125	126	127	130
Mean stack temperature [°C]		19	21	23	23	24	25	25	26	28	29	29	31	33	31	31	32	33
Diluate tank volume [L]		190	187	185	184	183	181	180	179	178	176	174	172	171	170	169	166	165
Concentrate tank volume [L]		19	22	24	24	26	27	27	28	30	32	33	34	36	37	38	40	42
Diluate composition[mg/dm^3]	**Cl^-**	30200			18500			18400			12490			9630			7200	5740
	SO_4^{2-}	200			227			198			181			153			129	102
	Na^+	18000			11400			11710			7980			6190			4650	3710
	K^+	275			124			112			82			65			53	46
	Mg^{2+}	12			< 10			< 10			< 10			< 10			< 10	< 10
	Ca^{2+}	49			21			18			12			11			< 10	< 10
Concentrate composition[mg/dm^3]	**Cl^-**	30400			71400			83800			93100			98600			100600	100700
	SO_4^{2-}	201			457			597			799			1028			1220	1282
	Na^+	18200			42900			50000			55700			58800			59200	59200
	K^+	276			791			903			960			959			920	899
	Mg^{2+}	12			29			35			39			40			< 50	< 50
	Ca^{2+}	49			148			173			182			181			168	167

Table 15 The results of batch-mode electrodialysis, current density 519 A/m^2, diluate:concentrate initial volume ratio 12.7:1

Time [h]		0	0.5	1	1.5	2	2.5	3	3.5	4	4.5	5	5.5	6
Stack voltage drop [V]		22.7	20	19.3	19.2	19.7	20.1	21.1	24.3	35	35	35	35	35
Applied current [A]		40	40	40	40	40	40	40	40	36.8	32.3	29.8	26.3	23.8
Diluate inlet flow rate [L/h]		81	96	97	102	105	108	109	110	114	114	114	114	114
Diluate outlet flow rate [L/h]		76	88	89	92	95	96	98	99	102	102	104	105	106
Concentrate inlet flow rate [L/h]		98	109	102	108	106	108	111	112	97	99	99	100	100
Concentrate outlet flow rate [L/h]		106	117	111	118	118	119	121	124	111	114	112	112	111
Mean stack temperature [°C]		19	22	22	24	25	27	28	30	31	32	33	33	33
Diluate tank volume [L]		190	186	182	178	172	168	162	158	151	148	145	142	140
Concentrate tank volume [L]		15	17	21	25	30	34	38	44	49	51	54	56	57
Diluate composition[mg/dm^3]	**Cl^-**	21600		17000		12100		6630		1960	2000	2720	1500	1370
	SO_4^{2-}	51		69		74		53		16	25	18	17	20
	Na^+	18800		11100		7880		4330		1280	1310	1770	980	900
	K^+	277		114		71		36		15	17	13	13	12
	Mg^{2+}	< 10		< 10		< 10		< 10		< 10	< 10	< 10	< 10	< 10
	Ca^{2+}	29		10		< 10		< 10		< 10	< 10	< 10	< 10	< 10
Concentrate composition[mg/dm^3]	**Cl^-**	29800		72600		80700		83000		85000	82600	83500	#####	80300
	SO_4^{2-}	70		410		558		710		887	940	993	1020	1032
	Na^+	19200		47000		52400		53900		55300	53800	54400	#####	52100
	K^+	283		890		970		947		865	837	837	816	796
	Mg^{2+}	10		43		43		40		35	34	34	33	32
	Ca^{2+}	30		99		110		107		94	90	90	87	85

Table 16 The results of batch-mode electrodialysis, current density 584 A/m^2, diluate:concentrate initial volume ratio 12.7:1

Time [h]		0	0.5	1	1.5	2	2.5	3	3.5	4
Stack voltage drop [V]		22.3	23.2	22.2	22.9	26.3	30.3	35	35	35
Applied current [A]		45	45	45	45	45	45	40	25.5	19.6
Diluate inlet flow rate [L/h]		71	80	80	82	86	88	88	69	67
Diluate outlet flow rate [L/h]		65	69	69	71	73	74	74	58	58
Concentrate inlet flow rate [L/h]		63	60	63	66	60	46	44	25	17
Concentrate outlet flow rate [L/h]		73	72	76	78	75	62	60	40	30
Mean stack temperature [°C]		17	21	23	24	27	28	30	31	32
Diluate tank volume [L]		190	184	179	175	169	164	157	151	145
Concentrate tank volume [L]		15	19	24	28	35	39	46	51	56
Diluate composition[mg/dm^3]	**Cl^-**	20800		14600		7920		1920	1130	790
	SO_4^{2-}	2660		148		70		17	22	28
	Na^+	19000		9520		5150		1260	810	530
	K^+	276		90		34		10	<10	< 10
	Mg^{2+}	14		< 10		< 10		< 10	< 10	< 10
	Ca^{2+}	38		< 10		< 10		< 10	< 10	< 10
Concentrate composition[mg/dm^3]	**Cl^-**	20800		56100		60100		59200	53800	50400
	SO_4^{2-}	2660		1390		1810		1960	1080	1810
	Na^+	19000		49900		54200		53600	47400	43900
	K^+	276		885		911		824	698	637
	Mg^{2+}	14		41		38		< 25	< 25	< 25
	Ca^{2+}	38		122		121		101	62	78

Table 17 The results of batch-mode electrodialysis, current density 649 A/m^2, diluate:concentrate initial volume ratio 12.7:1

Time [h]		0	0.5	1	1.5	2	2.5	3
Stack voltage drop [V]		33.1	25.8	25	24.5	24.7	25.4	35
Applied current [A]		50	50	50	50	50	50	46.8
Diluate inlet flow rate [L/h]		108	107	111	113	118	120	108
Diluate outlet flow rate [L/h]		99	100	104	106	110	112	94
Concentrate inlet flow rate [L/h]		75	96	100	102	105	107	80
Concentrate outlet flow rate [L/h]		83	105	109	111	115	115	87
Mean stack temperature [°C]		15	18	21	23	25	27	31
Diluate tank volume [L]		191	188	183	178	175	171	165
Concentrate tank volume [L]		15	17	22	25	28	32	37
Diluate composition[mg/dm^3]	**Cl^-**	20300		14400		11500		3480
	SO_4^{2-}	568		115		113		57
	Na^+	17700		9380		7510		2290
	K^+	257		94		63		24
	Mg^{2+}	11		< 10		< 10		< 10
	Ca^{2+}	32		10		< 10		< 10
Concentrate composition[mg/dm^3]	**Cl^-**	20300		57100		64200		65600
	SO_4^{2-}	568		928		1020		1210
	Na^+	17700		50500		58400		60500
	K^+	257		921		1010		944
	Mg^{2+}	11		< 25		27		26
	Ca^{2+}	32		111		122		114

The data collected during the batch tests have been used to develop empirical and semi-empirical models describing the investigated unit operations. Based on the electrodialysis tests, following model was established:

$$J_w = a_0 i \quad (1)$$

Where J_w is the water transport per single cell pair [$m^3/(m^2 s)$], a_0 = (1.66 ± 0.08)·10^{-9} $m^3/(A \cdot s)$, i is the current density [A/m^2].

The ion transport of i-th ion was described using the equation:

$$J_i = a_{1,i} \Delta C_i + a_{2,i} C_i^{d,out} i \quad (2)$$

Where J_i is the ion flux per single cell pair [$mol/(m^2 s)$], $C_i^{d,out}$ is the diluate concentration of i-th ion, and the empirical coefficients a_2 and a_3 are presented in Table 18, ΔC_i is the mean concentration difference of i-th ion, defined as:

$$\Delta C_i = \frac{C_i^{d,in} + C_i^{d,out}}{2} - \frac{C_i^{c,in} + C_i^{c,out}}{2} \quad (3)$$

Where $C_i^{d,in}$, $C_i^{d,out}$, $C_i^{c,in}$, $C_i^{c,out}$ denote, respectively, chloride concentration [mol/m^3] in the inlet of diluate compartment, outlet of diluate compartment, inlet of concentrate compartment, outlet of concentrate compartment.

Table 18 Parameters for the ED model

Coefficient		Value	Unit
a_0		1.66	10^9 $m^3/(A \cdot s)$
a_1	Cl^-	-3.36	10^7 m/s
a_2		1.39	10^6 $m^6/(A \cdot mol \cdot s)$
a_1	SO_4^{2-}	-16.8	10^7 m/s
a_2		7.62	10^6 $m^6/(A \cdot mol \cdot s)$
a_1	Na^+	-3.86	10^7 m/s
a_2		14.8	10^6 $m^6/(A \cdot mol \cdot s)$
a_1	K^+	-86.8	10^7 m/s
a_2		26.8	10^6 $m^6/(A \cdot mol \cdot s)$
a_1	Mg^{2+}	-17.1	10^7 m/s
a_2		2.98	10^6 $m^6/(A \cdot mol \cdot s)$
a_1	Ca^{2+}	0.66	10^7 m/s
a_2		28.1	10^6 $m^6/(A \cdot mol \cdot s)$

f. Magnesium hydroxide recovery by CrIEM

The precipitation of magnesium hydroxide by UNIPA's CrIEM crystallizer (BCr-3 equipment from Italian BEC) was tested using samples of 1st pass nanofiltration retentate collected at 70% and 80% of permeate recovery.

Samples of 1st pass nanofiltration retentate working at the pilot plant in "Bolesław Śmiały" coal mine were collected at 70% and 80% of permeate recovery and used for the test. The composition of feeds is presented in Table 19.

Table 19 The composition of feed samples used for CrIEM tests.

Feed	Permeate recovery	Ionic composition				
		Na^+	Mg^{2+}	Ca^{2+}	Cl^-	SO_4^{2-}
NF1-70%	70%	14.62	0.74	0.70	19.13	0.36
NF1-80%	80%	16.31	1.13	1.12	19.85	no data

Each test consists of two steps: start-up and feed&bleed (see Figure 23) experiment. First, 1L of NF retentate was placed in the buffer tank and 2 L of $Ca(OH)_2$ suspension was placed in another vessel. Both solutions were recirculated inside the crystallizer until all magnesium reacted. A pH-meter was used to check the course of the reaction.

Next, when the reaction ended and $Mg(OH)_2$ precipitated in the bottom part of conical buffer tank, the fresh NF retentate was pumped to the top of buffer tanks, while the magnesium hydroxide suspension was being removed from the bottom. Sampling was carried out at regular intervals.

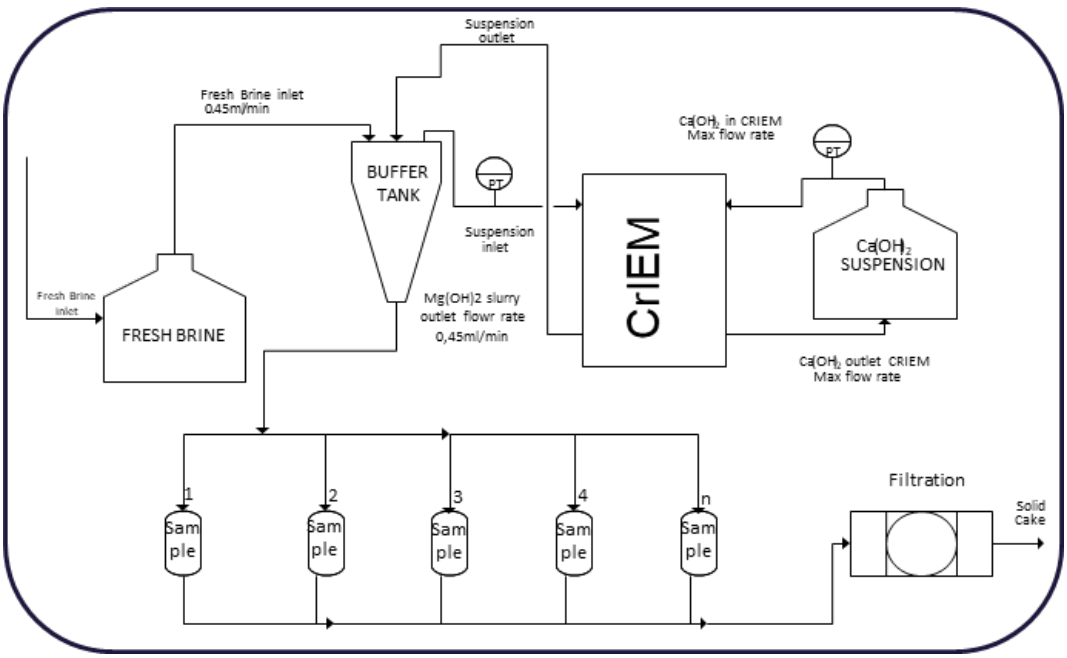

Figure 23 The general scheme of feed & bleed process

Every sample was filtered. The filtrates and the solid were analysed with EDTA titration. For solids analysis, 40 mg of it was dissolved in 100 ml of HCl 1M. The composition of obtained solid $Mg(OH)_2$ was analysed using thermogravimetric method (TGA), which showed that the sample contains 3.38% H_2O and pure $Mg(OH)_2$ (which decomposes) – see Figure 24. The obtained results are presented in the Table 20. The results confirmed that NF1 retentate stream can be used for magnesium hydroxide recovery and the CrIEM method can be used for that.

Table 20 Results obtained in the CrIEM test

Experiments with NF retentate collected at 70% permeate recovery							
Sample	Filtrate concentration [g/L]		Conversion [%]	Solid analysis		Sample volume [mL]	Magma density [g/L]
	Ca^{2+}	Mg^{2+}		Ca [%]	Mg [%]		
S1	0.5	0.05	93.1	7.6	92.4	300	2.01
S2	0.56	0.08	88.9	5.3	94.7	300	0.68
S2	0.55	0.12	83.4	3.8	96.2	300	0.79
S4	0.52	0.14	80.1	11.5	88.5	240	0.4
S5	0.57	0.06	91.3			240	0.04
S6	0.59	0.07	90.6			240	0.37
S7	0.61	0.01	99	1.2	98.8	2000	1.42
Experiments with NF retentate collected at 80% permeate recovery							
Sample	Filtrate concentration [g/L]		Conversion [%]	Solid analysis		Sample volume [mL]	Magma density [g/L]
	Ca^{2+}	Mg^{2+}		Ca [%]	Mg [%]		
S1	1.00	0.07	94.1	2.4	97.6	1000	0.66
S2*	0.34	0.09	92.5	15.6	79.6	1000	0.98
S2	1.00	0.00	100.0	0.0	100.0	800	1.94
S4	0.96	0.07	94.1	3.8	96.2	850	2.27

* sample contaminated with tap water

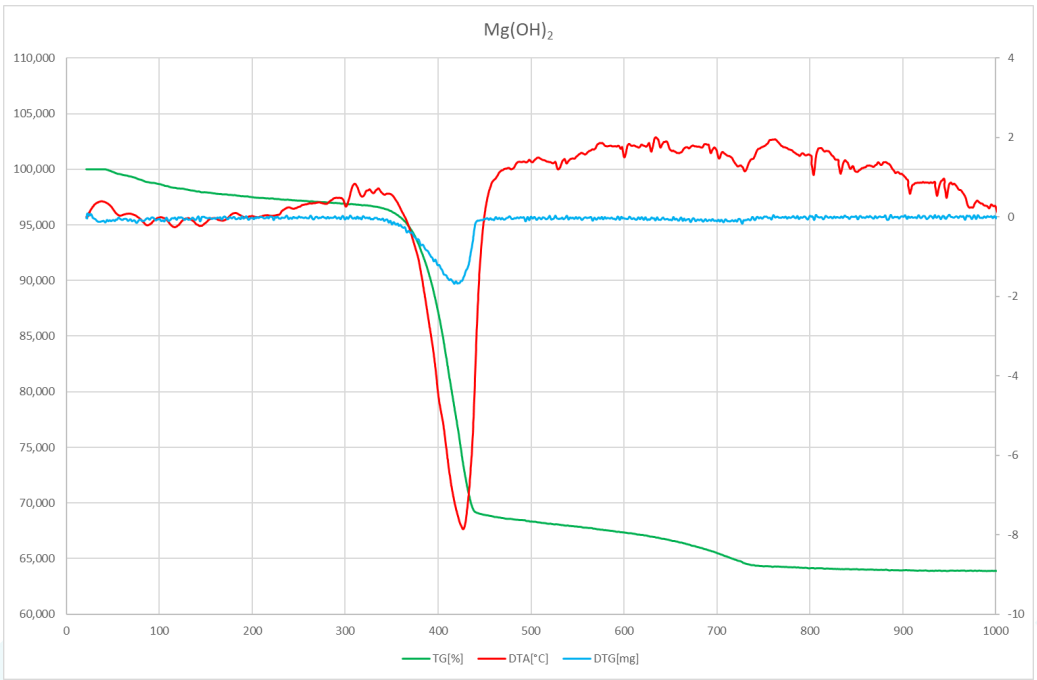

Figure 24 Results of the TGA test of the solid sample

g. Magnesium hydroxide recovery by roasted dolime suspension

Roasted dolime suspension was prepared by roasting JKSM dolomite of granulation 0.25 mm at 1200°C for 3.5 h. The roasted dolomite was analysed by a thermogravimetric method, which confirmed the correct preparation of the material. The magnesium hydroxide precipitation was performed in the 19 dm^3 CSTR crystallizer of hydraulic residence time of 0.5 h, which was fed the 10% water suspension of dolime (1.2 dm^3/h) and the 1st nanofiltration retentate containing 0.815 g/dm^3 of Mg^{2+} (35.2 dm^3/h). The pH of the reaction mixture was kept between 10-11. The sedimentation rate of $Mg(OH)_2$ was 120 cm/h. The obtained magnesium hydroxide slurry was vacuum filtered at 800 mBar. The filtration cake was washed with distilled water and dried at 105°C. The average filtration rate was 6.79 $kg/(m^2h)$. The composition of obtained MgO is presented in Table 21.

Table 21 The composition of the MgO sample obtained by precipitation by roasted dolime suspension

Compound	Mass fraction [%]
CaO	0.87
Na_2SO_4	0.18
B_2O_3	0.10
MnO	0.11
SiO_2	0.26
Fe_2O_3	0.46
Al_2O3	0.11
Cr_2O_3	0.0011
TiO_2	0.014
MgO	97.89

h. Eutectic freeze crystallization of sodium chloride

Crystallization of sodium chloride from the brine generated by NF-RO-ED system working on the coal mine water was tested using eutectic freeze crystallizer (EFC) – equipment BCr-1 from the Dutch BEC. The brines generated in the coal mine pilot plant up to this date were not, however suitable for crystallization, as the construction of electrodialysis still required optimization and was not working under required process conditions (too high concentrate flow and too low current density). Based on the ionic compositions of process streams, the compositions of the brines which should be produced in the systems were estimated, assuming the fluxes of bivalent ions are proportional to the fluxes of univalent ions – see Table 22.

Table 22 The composition of model solutions used in the EFC experiments

	Feed 1	Feed 2	Feed 3
Cl^- [g/dm^3]	180	180	180
Mg^{2+} [g/dm^3]	2.14	1.12	0.033
Ca^{2+} [g/dm^3]	6.97	2.97	0.035
SO_4^{2-} [g/dm^3]	0.507	0.264	0.277

A 2 L sample of each of the synthetic brine solutions were fed to a batch-mode eutectic freeze crystallizer equipped with mechanical stirrer (70 rpm) and a cooling jacket connected to an external cooler. The temperature inside was gradually lowered. After the eutectic point was reached, which was detected by lack of temperature change inside the reactor despite lowering the coolant temperature, ice crystals were added to the reaction mixture to precipitate/confirm ice crystals forming inside. When the occurrence of eutectic crystallization was

confirmed, samples of salt crystals, ice, and post-crystallization lyes were collected. The salt crystals were subjected to vacuum filtration and washed with 26.4% w/w sodium chloride solution. The filtrate from each washing was collected. The concentration of sodium, calcium, and magnesium was determined using ICP-MS method, whereas the concentration of chlorides and sulphates was determined by ion chromatography.

Table 23 for the ionic composition of collected liquid samples. The eutectic points were reached at -21.8°C, -21.5°C, and -21.2°C. The results have shown that eutectic freeze crystallization technology, as developed in the ZERO BRINE project, can be used in the production of salt even if the feed is highly contaminated with bivalent impurities.

Table 23 The composition of liquid samples collected during the EFC experiments on synthetic solutions

Sample	Concentration [g/L]				
	Na^+	Cl^-	SO_4^{2-}	Ca^{2+}	Mg^{2+}
Feed 1, initial brine	155.7	204.1	0.458	8.316	2.903
Feed 1, post-crystallization lye	153.0	185.7	0.513	12.163	3.342
Feed 2, initial brine	169.5	209.0	0.219	4.484	1.675
Feed 2, filtrate before washing	152.0	193.4	0.227	4.136	1.749
Feed 2, filtrate after 1st washing with saturated NaCl	180.1	220.3	<0.002	2.530	0.364
Feed 2, filtrate after 2nd washing with saturated NaCl	186.0	224.0	<0.002	1.213	0.141
Feed 2, filtrate after 3rd washing with saturated NaCl	187.0	227.0	<0.002	0.274	0.070
Feed 3, initial brine	166.0	207.3	0.230	1.142	0.082
Feed 3, filtrate before washing	159.8	194.2	0.244	1.619	0.084
Feed 3, filtrate after 1st washing with saturated NaCl	177.4	218.2	0.039	1.133	0.061
Feed 3, filtrate after 2nd washing with saturated NaCl	186.2	220.1	<0.002	1.158	0.051

4. Optimization of process conditions and comparison of energy consumption with reference plant

In order to assess the technology proposed in the ZERO BRINE project, following case studies have been modelled:

1) the feed water from the “Bolesław Śmiały” coal mine is pre-concentrated with reverse osmosis, then subjected to the vapour compression (VC) which concentrates it to 290 g/dm^3 as NaCl – this is the reference technology, which is currently utilized in the “Dębieńsko” desalination plant. According the reference plant staff, the energy consumption in this technology is 5 kWh/m^3 of treated brine in the RO and 44 kWh/m^3 of distillate in the VC.

2) the feed water from the “Bolesław Śmiały” coal mine is fed to the ultrafiltration and decarbonization, two-pass nanofiltration (NF1 working at 80%, NF2 working at 80% with all of the retentate recycled back to the NF1), then to RO-ED unit, which concentrates the brine up to ca. 111 g/L as Cl^-, then the ED concentrate is fed to the VC part of the “Dębieńsko” technology. The NF1 retentate is used for $Mg(OH)_2$ recovery using the CrIEM technology.

3) the feed water from the “Bolesław Śmiały” coal mine is fed to the ultrafiltration and decarbonization, two-pass nanofiltration (NF1 working at 80%, NF2 working at 80% with all of the retentate recycled back to the NF1), then to the RO-ED unit, which concentrates the brine up to ca. 111 g/L as Cl^-, then the ED concentrate is fed to the modern thermal method (MED of energy consumption of 12 kWh/m^3 of distillate, assuming no waste heat is available at the site). The NF1 retentate is used for $Mg(OH)_2$ recovery using the CrIEM technology.

4) the feed water from the “Bolesław Śmiały” coal mine is fed to the ultrafiltration and decarbonization, then to the two-pass nanofiltration (NF1 recovery 75%, NF2 recovery 75%) with intermediate gypsum precipitation (a CSTR crystallizer with hydraulic residence time of 1-2 h, which is enough to allow spontaneous precipitation of gypsum down to ca. 164% saturation without adding chemicals). The NF2 permeate is fed to RO-ED unit, which concentrates the brine up to ca. 111 g/L as Cl-, then the ED concentrate is fed to the modern thermal method (MED of energy consumption of 12 kWh/m^3 of distillate, assuming no waste heat is available at the site).

The rejection coefficients and energy consumption of each individual unit operations of ZERO BRINE technology were based on the data obtained in the pilot studies. Salt recovery was calculated assuming “Dębieńsko” crystallization technology, in which the amount of crystallized salt is limited by the bivalent impurities present The methodology of calculating crystallizer energy consumption, amount of recoverable salt and the ionic composition of post-crystallization lyes have been presented in M. Turek et al., “Application of nanofiltration and electrodialysis for improved performance of a salt production plant”, Desalin. Water Treat. 64 (2017) 244-250 (http://dx.doi.org/10.5004/dwt.2017.11392):

1) The maximum concentration of bivalent ions in the post-crystallization lyes is 8% (w/w) as $MgCl_2$+$CaCl_2$ – this is the actual limit of the crystallizer in the existing plant.

2) The maximum chloride concentration in the post-crystallization lyes is 200 g/L.

3) The solubility product of calcium sulphate is 4.302·10-6 mol4dm-6 – value calculated based on the composition of post-crystallization lyes from the plant and corresponding to the temperature and ionic strength of the liquid in the existing crystallizer.

4) Rejection coefficients of a RO membrane used in “Dębieńsko” technology were assumed as follows: R_{Cl^-} = 99.22%, R_{Mg2+} = 99.90%, R_{Ca2+} = 99.85%, R_{SO42-} = 99.72%. For the “ZERO BRINE” technology, the ionic compositions of the process streams obtained during the plant operation were used.

5) The maximum total dissolved salts content (TDS) of the RO concentrate is 60 g/L.

The “Dębieńsko” crystallizer can recover gypsum, so this factor was also taken into account. Magnesium hydroxide recovery was calculated as the amount of recoverable magnesium hydroxide in the NF retentate stream, assuming 100% of Mg^{2+} ions can be precipitated as $Mg(OH)_2$ with the addition of sodium hydroxide – in the case of “Dębieńsko” it was assumed as 0% since this reference technology does not recover magnesium. Water recovery was assumed as ratio of mixed RO permeate and thermal method distillate to the inlet brine volume. Since setting the flow in the pilot plant relied on using pump by-passes, the energy consumption in nanofiltration and reverse osmosis were calculated using methodology presented in Turek et al., “Energy Consumption and Gypsum Scaling Assessment in a Hybrid Nanofiltration- Reverse Osmosis-Electrodialysis system”, Chem. Eng. Technol. 41 (2018) 392-400 (http://dx.doi.org/10.1002/ceat.201700371), however instead

of relying upon theoretical rejection coefficients and pressures, real values obtained during continuous plant run were put into the equations:

$$E_{NF1} = \left(\frac{0.02724 P_{NF1}}{0.88 \cdot 0.94 \cdot Y_{NF1}} + 0.05\right)\left(\frac{V_{p,NF1}}{V_f}\right) \quad (4)$$

$$E_{NF2} = \left(\frac{0.02724 P_{NF2}}{0.88 \cdot 0.94 \cdot Y_{NF2}} + 0.05\right)\left(\frac{V_{p,NF2}}{V_f}\right) \quad (5)$$

$$E_{RO} = \left(\frac{0.02724 P_{RO}}{0.88 \cdot 0.94 \cdot Y_{RO}} + 0.05\right)\left(\frac{V_{p,RO}}{V_f}\right) \quad (6)$$

Where E_{NF1}, E_{NF2}, E_{RO} is the energy consumption of 1st pass nanofiltration, 2nd pass nanofiltration, and reverse osmosis, respectively, P_{NF1}, P_{NF2}, P_{RO} are the average feed pressure observed at set recovery in 1st pass nanofiltration, 2nd pass nanofiltration, and reverse osmosis, respectively, Y_{NF1}, Y_{NF2}, Y_{RO} are the permeate recovery of 1st pass nanofiltration (80%), 2nd pass nanofiltration (80%), and reverse osmosis, V_{NF1}, V_{NF2}, V_{RO}, V_f are the permeate flow rates of 1st pass nanofiltration, 2nd pass nanofiltration, reverse osmosis and feed water, respectively.

Similarly, in the case of electrodialysis, the energy consumption was calculated using measured values of voltage and current affecting the ED energy consumption (see Figure 22), and the ionic composition of the obtained streams:

$$E_{ED} = \sum \frac{E_{ED,c,i}\left(C_{c,out,i} V_{c,out,i} - C_{c,in,i} V_{c,in,i}\right)}{V_f} \quad (7)$$

Where $E_{ED,c,i}$ is the energy consumption in kWh/t of transported salt in the i-th electrodialyzer in the cascade (in the pilot plant i=2), as presented in Figure 22, $C_{c,out,i}$ and $C_{c,in,i}$ are the salt concentration in the concentrate inlet and outlet of i-th electrodialyzer, respectively, $V_{c,out,i}$ and $V_{c,in,i}$ are the volumetric flows of the concentrate inlet and outlet of i-th electrodialyzer, respectively.

Table 24 presents the calculated energy consumption and recovery of raw materials. The results suggest that the application of intermediate gypsum precipitation is necessary in order to improve performance in comparison with the existing technology. The salt recovery can be increased from 81 to over 92% with simultaneous cut in energy consumption by a third. Additionally, the ZERO BRINE technology allows for the recovery of magnesium hydroxide.

Table 24 Comparison of energy consumption and recovery of raw materials in the reference "Dębieńsko" technology and the variants of the proposed ZERO BRINE technology.

Technology	Energy consumption [kWh/m^3 of treated brine]	Bivalent impurities in the concentrate stream [g/dm^3 as Ca+Mg]	Salt recovery [%]	Magnesium hydroxide recovery [%]	Water recovery (not including crystallizer) [%]	Recovered gypsum [kg/m^3 of treated brine]
"Dębieńsko"	16.7	8.25	81.0	0	92.4	1.36
"ZERO BRINE" coupled with "Dębieńsko" evaporator	12.9	0.036	56.9	96.7	75.7	0.002
"ZERO BRINE" coupled with modern evaporator and crystallizer	12.0	0.036	56.9	96.6	75.7	0.002
"ZERO BRINE" with intermediate gypsum precipitation and modern evaporator	11.2	0.104	92.8	94.9	90.6	0.84

5. Conclusions

Following conclusions can be drawn based on the data obtained during the pilot studies:

1) nanofiltration can be safely operated at high permeate recovery (80%), without the observable scaling,

2) two-pass nanofiltration system has shown very high rejection coefficients with respect two bivalent ions, even above 95% (see Table 5), and relatively low rejection coefficients of univalent ions, which is a desired behaviour from the point of view of separating sodium chloride from calcium and magnesium. The results confirm that from the point of view of circular economy, the application of nanofiltration is very desirable, as it would not be possible to subsequently recover magnesium hydroxide or gypsum without selective removal of bivalent salts from the feed water.

3) electrodialysis working on the reverse osmosis retentate can exhibit relatively low energy consumption (even around 300-400 kWh/t of transported salt, see Figure 22), which makes it a feasible method for decreasing the volume of saline waste water from desalination plants.

4) it was not possible to reach the desired goal of producing the concentrated brine directly in the electrodialysis. This can be a result of using dense intermembrane spacers (commercial 0.35 mm PC-Cell spacers) with thick membranes. Although the SUT has a laboratory-scale technology of thinner spacers, application of which can generate concentrated brine as confirmed by laboratory tests, upscaling the technology met unforeseen technical difficulties which could not be resolved in time for pilot tests. Further investigations are pending,

5) the application of intermediate gypsum precipitation in the two-pass nanofiltration is a necessary step in order to achieve salt recovery higher than the reference “Dębieńsko” technology,

6) the energy consumption of the proposed “ZERO BRINE” technology is substantially lower (23-33%) than the reference “Dębieńsko” technology, reaching 11.2 kWh/m^3 of treated brine,

7) the proposed “ZERO BRINE” technology can increase the recovery of valuable raw materials by increasing the salt recovery and allowing for the recovery of magnesium hydroxide,

8) the proposed “ZERO BRINE” technology should include a modern evaporator as the last step before crystallization in order to decrease the energy consumption,

9) the proposed variant of the “ZERO BRINE” technology is as follows: the brine pretreated with ultrafiltration is subjected to the first pass of nanofiltration (NF1); the permeate is subjected to a second pass of nanofiltration (NF2). The NF1 and NF2 retentates are passed through gypsum precipitation and magnesium recovery units; after recovery of $Mg(OH)_2$ and $CaSO_4$, 90% of the stream is recycled before NF1. The NF2 permeate is fed to the hybrid reverse osmosis (RO)-electrodialysis (ED) unit, from which the RO permeate is recovered, the ED concentrate is fed to a modern evaporator (MED), the ED diluate is recycled back to RO.